

# Model selection-based estimation for generalized additive models using mixtures of g-priors: Towards systematization

Gyeonghun Kang<sup>1</sup> and Seonghyun Jeong<sup>\*,2,3</sup>

<sup>1</sup>Department of Statistical Science, Duke University, Durham, North Carolina, USA

<sup>2</sup>Department of Statistics and Data Science, Yonsei University, Seoul, Korea

<sup>3</sup>Department of Applied Statistics, Yonsei University, Seoul, Korea

December 13, 2023

## Abstract

We consider the estimation of generalized additive models using basis expansions coupled with Bayesian model selection. Although Bayesian model selection is an intuitively appealing tool for regression splines, its use has traditionally been limited to Gaussian additive regression because of the availability of a tractable form of the marginal model likelihood. We extend the method to encompass the exponential family of distributions using the Laplace approximation to the likelihood. Although the approach exhibits success with any Gaussian-type prior distribution, there remains a lack of consensus regarding the best prior distribution for nonparametric regression through model selection. We observe that the classical unit information prior distribution for variable selection may not be well-suited for nonparametric regression using basis expansions. Instead, our investigation reveals that mixtures of g-priors are more suitable. We consider various mixtures of g-priors to evaluate the performance in estimating generalized additive models. Furthermore, we conduct a comparative analysis of several priors for knots to identify the most practically effective strategy. Our extensive simulation studies demonstrate the superiority of model selection-based approaches over other Bayesian methods.

*Keywords:* Bayesian nonparametrics; exponential family models; mixtures of g-priors; nonparametric regression; regression splines.

## 1 Introduction

Since its inception, the generalized additive model (GAM) has played a significant role in statistics and machine learning, and has received a great deal of attention from many theorists and practitioners. The GAM is seen as an interpretable semiparametric compromise between the parametric generalized linear model (GLM) and fully nonparametric regression with multidimensional smoothing. More specifically, the GAM explains the relationship between multiple predictor variables and a (possibly non-Gaussian) response variable by employing an additive structure of univariate functions (Hastie and Tibshirani, 1986). Therefore, at the expense of the

---

\*Corresponding author: sjeong@yonsei.ac.kr

flexibility of multidimensional smoothing, the GAM provides a straightforward interpretation of the amount each predictor variable contributes to the mean response as a univariate function.

A variety of estimation procedures have been proposed for nonparametric regression and additive models from frequentist and Bayesian perspectives. Focusing on the Bayesian philosophy, typical techniques for univariate smooth function estimation include Gaussian process priors (Williams and Rasmussen, 1995), Bayesian P-splines (Lang and Brezger, 2004), and basis expansion methods with model selection (Smith and Kohn, 1996; Denison et al., 1998; DiMatteo et al., 2001). As a branch of Bayesian estimation methods, basis expansion with Bayesian model selection (BMS), which we call the BMS-based approach to nonparametric regression, enjoys appealing theoretical properties and successful empirical performances (Smith and Kohn, 1996; Denison et al., 1998; DiMatteo et al., 2001; Rivoirard and Rousseau, 2012; De Jonge and Van Zanten, 2012; Shen and Ghosal, 2015). Specifically, the BMS-based approaches determine intrinsic basis terms by comparing Bayes factors based on BMS, which translates to choosing more plausible basis terms among possible candidates in a data-driven manner.

Although the BMS-based methods are conceptually simple, their computational efficacy is contingent upon the accessibility of calculating the marginal likelihood. This limitation has typically confined the application of BMS to Gaussian regression within nonparametric regression. In the context of GLMs and GAMs, marginalization is often unachievable unless a conjugate prior is used for the coefficients. However, such a conjugate prior does not provide a convenient form of the marginal likelihood (Chen and Ibrahim, 2003). The most accessible scenario may be when there are available expressions involving latent variables, such as in logistic and probit regression (e.g., Jeong et al., 2017; Sohn et al., 2023). If marginalization is not analytically tractable, the BMS-based methods require numerical marginalization of the coefficients through Markov chain Monte Carlo (MCMC) algorithms, such as the reversible jump MCMC (Green, 1995). These are often far more inefficient than using Bayes factors, unless a sound proposal distribution is available. This challenge has contributed to the prevalence of the P-spline-based Bayesian methods for estimation in GAMs during the early stages of their development (e.g., Fahrmeir and Lang, 2001; Brezger and Lang, 2006).

One natural solution to address this issue involves considering an approximation to the likelihood, such as the Laplace approximation, enabling the calculation of the marginal likelihood with a Gaussian prior distribution on the coefficients (Li and Clyde, 2018). This allows us to employ the BMS-based approaches for estimation in GAMs with distributions belonging to the exponential family. The approximation idea has occasionally been used for the BMS-based approaches (e.g., DiMatteo et al., 2001), and has been widely accepted in the literature on GAM estimation with Bayesian P-splines for computational efficiency (Sabanés Bové et al., 2015; Gressani and Lambert, 2021).

When a Gaussian or Gaussian mixture prior is used for the coefficients, the Laplace approximation in BMS-based GAM estimation facilitates the straightforward derivation a closed-form expression of the marginal likelihood. However, it remains unclear which prior distribution is best for our purpose of basis determination. In the literature on variable selection, it has been continually reported that mixture priors outperform the classical Gaussian prior called Zellner's g-prior and its variants (Liang et al., 2008; Li and Clyde, 2018). Such mixture priors, also known as mixtures of g-priors, have many desirable properties and resolve the paradoxes of the g-prior

(Liang et al., 2008). Various mixtures of g-priors have been proposed under the framework of linear regression (e.g., Zellner and Siow, 1980; Liang et al., 2008; Maruyama and George, 2011; Bayarri et al., 2012; Womack et al., 2014), and there have been a few attempts to extend them for the GLM (Sabanés Bové and Held, 2011; Held et al., 2015; Fouskakis et al., 2018). Recently, Li and Clyde (2018) provided a comprehensive and extended framework for mixtures of g-priors for the GLM. However, the best-performing mixture prior for the BMS-based GAM estimation remains unknown. To address this, understanding the influence of mixtures of g-priors on penalizing nonparametric functions is essential. Even in the context of Gaussian additive regression, determining the best mixture prior remains uncertain.

Another crucial aspect of prior specification for the BMS-based methods involves the choice of a prior distribution for intrinsic basis terms. Given that spline basis functions are often fully determined by knot locations, this naturally translates into a prior on knots. Various prior distributions have been proposed to strike a balance between computational convenience and estimation quality (e.g., Smith and Kohn, 1996; Denison et al., 1998; DiMatteo et al., 2001; Shen and Ghosal, 2015). Existing prior distributions on knots can be categorized into a few classes based on the principles underlying their constructions; generally, the more flexible the prior, the better the approximation, but with a greater computational burden. Unfortunately, it remains unclear which class of prior distributions is most suitable for determining the best spline knots.

The contributions of this study are threefold. First, we systematize BMS-based approaches for Generalized Additive Model (GAM) estimation using the Laplace approximation and a unified framework for mixtures of g-priors as proposed by Li and Clyde (2018). In doing so, we enhance computational efficiency by introducing a new form of natural cubic spline functions tailored for the BMS-based approaches. Second, among various mixtures of g-priors belonging to a general class, we determine a default mixture prior for GAM estimation. In pursuit of this, we enhance our understanding of how mixtures of g-priors penalize the model during GAM estimation. The empirical performance of various mixture priors is also scrutinized through an extensive simulation study. Our experience indicates that a traditional g-prior directly utilizing the sample size, also known as the unit information prior (Kass and Wasserman, 1995), may not be suitable, and a mixture of g-priors should be used instead. Lastly, we categorize the prior distributions for knots available in the literature into three groups and examine which class is the best for GAM estimation. Our investigation indicates that a prior distribution that is well-balanced between flexibility and accessibility performs the best. Specifically, the most flexible prior, known as the free-knot spline (Denison et al., 1998; DiMatteo et al., 2001), is excessive for GAM estimation in practice, whereas a less flexible but computationally friendly approach based on variable selection (Smith and Kohn, 1996) shows successful empirical results with fast mixing. We support our claims with a verity of numerical results. An R package that implements the sampling algorithms for our GAM estimation is available on the first author's GitHub.<sup>1</sup>

The remainder of this paper is structured as follows. Section 2 introduces the basic construction of GAMs using a spline basis expansion with natural cubic splines. Section 3 describes mixtures of g-priors for BMS under a unified framework, and compares the mixture priors for estimation of GAMs by interpreting them as penalty functions for nonparametric regression. In

---

<sup>1</sup><https://github.com/hun-learning94/gambms>

Section 4, we categorize the available prior distributions on knots into three different strategies for the BMS-based approaches. In Section 5, comprehensive simulation and numerical studies are performed to determine the best prior distribution and to compare the BMS-based approaches with their Bayesian competitors for GAM estimation. Section 6 demonstrates the application of the BMS-based method to the Pima diabetes dataset. Lastly, Section 7 concludes the study with a discussion. The supplementary material includes proofs of the propositions, additional simulation studies, and instructions for installing our R package.

## 2 Generalized additive models via basis expansion

For given predictor variables  $x_i = (x_{i1}, x_{i2}, \dots, x_{ip})^T \in \mathbb{R}^p$ , suppose that a response variable  $Y_i \in \mathbb{R}$  has a distribution belonging to the exponential family; that is, the density of  $Y_i$  is

$$y_i \mapsto p(y_i; \theta_i, \phi) = \exp \left( \frac{y_i \theta_i - b(\theta_i)}{\phi} + c(y_i, \phi) \right), \quad i = 1, \dots, n, \quad (1)$$

where  $\theta_i$  is a natural parameter modeled by  $x_i$ ,  $\phi$  is a scale parameter, and  $b$  and  $c$  are known functions. The dependency of  $\theta_i$  on  $x_i$  is clarified below. Although we mainly focus on the case in which the dispersion parameter  $\phi$  is known, we also consider Gaussian regression with unknown  $\phi$  in Section S5 of the supplementary material. Assuming that  $b$  is twice differentiable and  $b''(\theta_i) > 0$ , the expected value and variance of  $Y_i$  are given by  $E(Y_i) = b'(\theta_i)$  and  $Var(Y_i) = \phi b''(\theta_i)$ , respectively. We choose a monotonically increasing link function  $h$  that parameterizes the natural parameter as  $\theta_i = (h \circ b')^{-1}(\eta_i)$ , where  $\eta_i$  is an additive predictor expressed as

$$\eta_i = \alpha + \sum_{j=1}^p f_j(x_{ij}), \quad i = 1, \dots, n, \quad (2)$$

with a global mean  $\alpha$  and univariate functions  $f_j : \mathbb{R} \rightarrow \mathbb{R}$ ,  $j = 1, \dots, p$ . To ensure the identifiability, the functions  $f_j$  are assumed to satisfy  $\sum_{i=1}^n f_j(x_{ij}) = 0$ ,  $j = 1, \dots, p$ .

For the complete model specification, the most important part is determining how to characterize the nonparametric functions  $f_j$ . Throughout this study, the functions  $f_j$  are parameterized using a spline basis representation. In this respect,  $f_j$  are expressed as linear combinations of  $K_j$  basis functions  $b_{j1}, \dots, b_{jK_j}$ ; that is, with coefficients  $\beta_{jk} \in \mathbb{R}$ ,

$$f_j(\cdot) = \sum_{k=1}^{K_j} \beta_{jk} b_{jk}(\cdot), \quad j = 1, \dots, p.$$

For the identifiability condition  $\sum_{i=1}^n f_j(x_{ij}) = 0$  to be satisfied, we assume that each basis function satisfies  $\sum_{i=1}^n b_{jk}(x_{ij}) = 0$ ,  $j = 1, \dots, p$ . This can be easily achieved by centering an unrestricted basis term  $b_{jk}^*$  as

$$b_{jk}(\cdot) = b_{jk}^*(\cdot) - \frac{1}{n} \sum_{i=1}^n b_{jk}^*(x_{ij}), \quad j = 1, \dots, p, \quad k = 1, \dots, K_j. \quad (3)$$

Let  $B_j \in \mathbb{R}^{n \times K_j}$  be a matrix whose  $(i, k)$ th component is  $b_{jk}(x_{ij})$ . The centering procedure is easily achieved by the projection  $B_j = (I_n - n^{-1} \mathbf{1}_n \mathbf{1}_n^T) B_j^*$  with an unrestricted basis matrix  $B_j^*$

defined with  $b_{jk}^*$  for its  $(i, k)$ th component. We define  $B = [B_1, \dots, B_p] \in \mathbb{R}^{n \times J}$  and a vector of full coefficients  $\beta = (\beta_{11}, \dots, \beta_{1K_1}, \dots, \beta_{p1}, \dots, \beta_{pK_p})^T \in \mathbb{R}^J$ , where  $J = \sum_{j=1}^p K_j$ . We then write a vector of additive predictors  $\eta = (\eta_1, \dots, \eta_n)^T$  as  $\eta = \alpha 1_n + B\beta$ .

Many classes of basis functions can be used for smooth function estimation. In this study, we deploy natural cubic spline basis functions to prevent erratic behavior of splines at the boundaries. This is equivalent to using any type of piecewise polynomial basis functions (including B-splines) with suitable natural boundary conditions, provided that a prior distribution is invariant to linear bijections of a design matrix. Specifically, for boundary knots  $\{t^L, t^U\}$  and the set of  $M$  interior knots  $\{t_1, \dots, t_M\}$  satisfying  $-\infty < t^L < t_1 < \dots < t_M < t^U < \infty$ , we define natural cubic spline basis functions  $N_k : \mathbb{R} \rightarrow \mathbb{R}$ ,  $k = 1, \dots, M + 1$ , as

$$\begin{aligned} N_1(u) &= u, \\ N_{k+1}(u) &= N(u; t^L, t^U, t_k) \\ &\equiv \frac{(u - t_k)_+^3 - (u - t^U)_+^3}{t^U - t_k} - \frac{(u - t^L)_+^3 - (u - t^U)_+^3}{t^U - t^L}, \quad k = 1, \dots, M. \end{aligned} \tag{4}$$

Along with the constant term  $N_0(u) = 1$ , the basis functions in (4) generate piecewise cubic functions. These functions are restricted as linear beyond the boundary knots  $\{t^L, t^U\}$ , resulting in increased stability near the boundaries caused by the induced constraints at  $\{t^L, t^U\}$ . The constant term is excluded in (4) because it is redundant given the intercept term. Our experience, consistent with well-known observations, indicates that the use of natural cubic splines significantly reduces estimation bias near the boundaries compared to cubic splines without natural conditions.

Although the basis construction in (4) is based on the truncated power series, our definition is slightly different from the form of truncated power natural cubic splines commonly used in the literature, for example, equations (5.4) and (5.5) in [Hastie et al. \(2009\)](#). It can be shown that the basis terms in (4) span the identical piecewise cubic polynomial space with natural boundary conditions. However, our definition in (4) has an additional favorable property where inserting a new knot-point  $t_* \in (t^L, t^U)$  simply leads to adding a new basis term defined as  $N(\cdot; t^L, t^U, t_*)$  into the set  $\mathcal{N} = \{N_k, k = 0, 1, \dots, M + 1\}$  without altering the current basis terms in  $\mathcal{N}$ . This property may not be present in other natural cubic spline basis functions, such as the natural cubic B-spline basis and the basis in equations (5.4) and (5.5) of [Hastie et al. \(2009\)](#). This is because a single basis term in those cases may depend on more than two knots, and inserting a knot-point may alter other basis terms. This characteristic makes our basis terms in (4) more attractive for model selection-based approaches (see Sections 4.2 and 4.3), as it enables faster computation by reducing the time spent on expanding the design matrix at each iteration. See Section S7 of the supplementary material for related simulation results. To our knowledge, this study is the first to utilize the form of natural cubic splines in (4). The properties are formalized in the following propositions.

**Proposition 1.** *The set  $\mathcal{N} = \{N_k, k = 0, 1, \dots, M + 1\}$  is a basis for the cubic spline space with natural boundary conditions.*

**Proposition 2.** *The addition of a new interior knot-point  $t_* \in (t^L, t^U)$  introduces a corresponding basis term  $N(\cdot; t^L, t^U, t_*)$  into  $\mathcal{N}$ . Similarly, the elimination of an existing interior knot-point*

$t_k \in t$  eliminates a corresponding basis term  $N(\cdot; t^L, t^U, t_k)$  in  $\mathcal{N}$ .

Proofs are provided in Section S2 of the supplementary material. We choose our basis terms  $b_{jk}^*$  using the natural cubic spline basis functions in (4). Specifically, using the observed design points, we set the boundary knots as  $\xi_j^L = \min_{1 \leq i \leq n} x_{ij}$  and  $\xi_j^U = \max_{1 \leq i \leq n} x_{ij}$  for each  $j$ . Then, with a given set of knots  $\xi_j = \{\xi_{j1}, \dots, \xi_{jL_j}\}$  satisfying  $\xi_j^L < \xi_{j1} < \dots < \xi_{jL_j} < \xi_j^U$ , the uncentered basis terms are chosen as

$$b_{j1}^*(\cdot) = N_1(\cdot), \quad b_{j,k+1}^*(\cdot) = N(\cdot; \xi_j^L, \xi_j^U, \xi_{jk}), \quad k = 1, \dots, L_j. \quad (5)$$

The class of spline functions is highly dependent on the specification of knots  $\xi = \{\xi_1, \dots, \xi_p\}$ . Hence, it is essential to choose a suitable knot placement to capture the local and global functional characteristics while avoiding overfitting. From the Bayesian point of view, one natural approach is to let the data choose the most appropriate knots  $\xi$  from a predetermined set  $\Xi$  via BMS. The idea has become widely accepted in the literature (e.g., [Smith and Kohn, 1996](#); [Denison et al., 1998](#); [DiMatteo et al., 2001](#); [Rivoirard and Rousseau, 2012](#); [De Jonge and Van Zanten, 2012](#); [Shen and Ghosal, 2015](#); [Jeong and Park, 2016](#); [Jeong et al., 2017](#)). A set  $\Xi$  can be a countable or uncountable collection of knots. A richer  $\Xi$  provides flexible estimation for the regression spline functions but may lead to computational inefficiency. Under the Bayesian framework, specifying  $\Xi$  using a predetermined law can be viewed as assigning a prior distribution on  $\xi$  over the infinite-dimensional space for all possible knot locations with restricted support  $\Xi$ . The key to success is how to put a prior on  $\xi$  with a suitably restricted support  $\Xi$ . Several possibilities for a prior on  $\xi$  will be discussed in Section 4.

An additional advantage of the formulation in (5) is that the fully linear relationship is also easily characterized by our specification. More precisely, if  $\xi_j$  is empty, the basis consists only of the linear term  $b_{j1}^*$ . This situation is especially beneficial when a predictor variable is binary or assumed to have a linear effect. In this scenario, we may simply set the corresponding  $\xi_j$  to be an empty set, which is viewed as assigning a point mass prior to empty  $\xi_j$ . As a result, generalized additive partial linear models (GAPLMs), with both parametric and nonparametric additive terms ([Wang et al., 2011](#)), are naturally subsumed by our construction without any modifications.

One of the main advantages of the BMS-based approaches to nonparametric regression is that they provide model-averaged estimates instead of resorting to a specific knot location. Our goal is to examine model-averaged estimates of a functional  $\mathcal{L} : (\alpha, f_1, \dots, f_p) \mapsto \mathcal{L}(\alpha, f_1, \dots, f_p)$  of interest, which is parameterized by the coefficients  $\alpha$  and  $\beta$ . For example, we may be interested in a pointwise evaluation of the additive predictor  $\alpha + \sum_{j=1}^p f_j(x_j)$  or the univariate functions  $f_j(x_j)$ ,  $j = 1, \dots, p$ , at some  $x = (x_1, \dots, x_p)^T$ . The model-averaged posterior of a functional is given by

$$\pi(\mathcal{L}(\alpha, f_1, \dots, f_p) | Y) = \int_{\Xi} \pi(\mathcal{L}(\alpha, f_1, \dots, f_p) | \xi, Y) d\Pi(\xi | Y). \quad (6)$$

A key to our Bayesian procedure is how to assign a prior distribution for model selection and how the posterior distribution of  $\xi$ ,  $\Pi(\xi | Y)$ , can be explored. In what follows, we write  $B_{\xi} = B$ ,  $\beta_{\xi} = \beta$ ,  $J_{\xi} = J$ , and  $\eta_{\xi} = \alpha 1_n + B_{\xi} \beta_{\xi}$  to emphasize the dependency on  $\xi$ . Observe that  $J_{\xi} = p + \sum_{j=1}^p |\xi_j|$ , where  $|\xi_j|$  is the number of knots  $\xi_j$ ,  $j = 1, \dots, p$ .

### 3 Mixtures of g-priors for generalized additive models

Our main objective is to explore the posterior distribution of a functional  $\mathcal{L}(\alpha, f_1, \dots, f_p)$ . To obtain a model-averaged estimate, we need to (numerically) evaluate the integration in (6), which requires exploring the posterior distribution  $\Pi(\alpha, \beta_\xi, \xi \mid Y)$ . Accordingly, we need to specify a prior distribution  $\Pi(\alpha, \beta_\xi, \xi)$  jointly over the parameter space. Possible priors for  $\xi$ ,  $\Pi(\xi)$ , will be discussed in Section 4. The remaining crucial part is determining a prior for the knot-specific coefficients  $\beta_\xi$ , that is,  $\Pi(\beta_\xi \mid \xi)$ , for which this study employs mixtures of g-priors. Here, we elucidate mixtures of g-priors for the BMS-based approaches to GAMs and the resulting posteriors. We also provide a toy example to understand how the mixture priors penalize GAMs.

#### 3.1 Mixtures of g-priors for exponential family models

We specify a prior distribution  $\Pi(\alpha, \beta_\xi \mid \xi) = \Pi(\alpha)\Pi(\beta_\xi \mid \xi)$ . Following the convention, we assign an improper uniform prior on the common parameter  $\alpha$ , that is,

$$\pi(\alpha) \propto 1. \quad (7)$$

The use of this improper prior has been justified in the literature (Berger et al., 1998; Bayarri et al., 2012). Next, we discuss  $\Pi(\beta_\xi \mid \xi)$ . For model selection in linear regression, Zellner's g-prior is often preferred because of its computational efficiency and invariance to linear transformations (Zellner, 1986). In our spline setup, invariance to transformations of a design matrix is particularly appealing because it is ideal for the procedure to remain invariant to a specific choice of basis functions, as long as a target spline space is correctly generated. In this sense, the invariance of the g-prior supports our spline basis system defined in (5) based on Proposition 1. Unfortunately, the computational advantage of the g-prior is generally lost in GAMs because Gaussian priors are not conjugate to non-Gaussian models, resulting in the inability to achieve a closed-form expression of the marginal likelihood  $p(Y \mid \xi)$ . The computation for the posterior distribution in (6) becomes more challenging without the calculation of the marginal likelihood. To address this issue, we consider approximating the likelihood using the Laplace approximation with a suitable variant of the g-prior. The Laplace approximation has occasionally been used for nonparametric regression with g-priors (e.g., DiMatteo et al., 2001).

For the function  $\theta = (h \circ b')^{-1}$ , let  $J_n(\hat{\eta}_\xi) = \text{diag}(-Y_i\theta''(\hat{\eta}_{\xi,i}) + (b \circ \theta)''(\hat{\eta}_{\xi,i}), i = 1, \dots, n)$  be the observed information matrix of  $\eta_\xi$  evaluated at  $\hat{\eta}_\xi$  (defined as the Hessian matrix of the negative log-likelihood), where  $\hat{\eta}_\xi = (\hat{\eta}_{\xi,1}, \dots, \hat{\eta}_{\xi,n})^T = \hat{\alpha}_\xi 1_n + B_\xi \hat{\beta}_\xi$  with the maximum likelihood estimators  $\hat{\alpha}_\xi$  and  $\hat{\beta}_\xi$  (assuming that  $\hat{\alpha}_\xi$  and  $\hat{\beta}_\xi$  exist). We restrict our attention to the case where  $J_n(\hat{\eta}_\xi)$  is positive definite. This is usually the case except for a few extreme situations such as the complete separation in logistic regression (Li and Clyde, 2018). Among the variants of the g-prior for the exponential family models, we deploy the following form proposed by Li and Clyde (2018),

$$\beta_\xi \mid g, \xi \sim N(0, g(\tilde{B}_\xi^T J_n(\hat{\eta}_\xi) \tilde{B}_\xi)^{-1}), \quad (8)$$

where  $g > 0$  serves as a dispersion factor controlling the prior influence, and  $\tilde{B}_\xi = [I_n - \text{tr}(J_n(\hat{\eta}_\xi))^{-1} 1_n 1_n^T J_n(\hat{\eta}_\xi)] B_\xi$  is the matrix consisting of the columns of  $B_\xi$  centered by the weighted

average with the diagonal elements of  $J_n(\hat{\eta}_\xi)$ . The prior in (8) requires  $\tilde{B}_\xi^T J_n(\hat{\eta}_\xi) \tilde{B}_\xi$  to be invertible. This is satisfied if and only if  $B_\xi$  is of full-column rank (observe that  $J_n(\hat{\eta}_\xi)$  is positive definite and  $\text{rk}(B_\xi) = \text{rk}(\tilde{B}_\xi)$ , where  $\text{rk}(\cdot)$  is the rank of a matrix.) Hence, the full-column rank condition will be made for  $\Pi(\xi)$  in Section 4. Although the prior in (8) can be extended by adopting a generalized inverse, we do not pursue this direction (see Section 2.5 of [Li and Clyde \(2018\)](#) for further discussion).

In addition to the prior in (8), there exist many other variants of the g-prior for the exponential family models (e.g., [Kass and Wasserman, 1995](#); [Hansen and Yu, 2003](#); [Gupta and Ibrahim, 2009](#); [Sabanés Bové and Held, 2011](#); [Held et al., 2015](#)). Here we adopt the prior in (8) because it provides a convenient expression for the approximate marginal likelihood. Moreover, our prior may better capture the large sample covariance structures and local geometry than other variants of the g-prior ([Li and Clyde, 2018](#)). It is worth mentioning that the prior in (8) is dependent on the observation vector  $Y$ , which shows it should be accepted by the empirical Bayes philosophy. Nonetheless, we suppress the dependency on  $Y$  in the expression of (8) for notational convenience.

Integrating the second order Taylor expansion for the likelihood with respect to (7) and (8), we obtain

$$p(Y | g, \xi) \approx p(Y | \hat{\eta}_\xi) \text{tr}(J_n(\hat{\eta}_\xi))^{-1/2} (g+1)^{-J_\xi/2} \exp\left(-\frac{Q_\xi}{2(g+1)}\right), \quad (9)$$

where  $p(Y | \hat{\eta}_\xi)$  is the likelihood evaluated at  $\hat{\eta}_\xi$  with given  $\xi$  and  $Q_\xi = \hat{\beta}_\xi^T \tilde{B}_\xi^T J_n(\hat{\eta}_\xi) \tilde{B}_\xi \hat{\beta}_\xi$  is the Wald statistic; see Section S3 of the supplementary material for the derivation of (9). The expression in (9) shows that if  $g$  is predetermined as a hyperparameter, the marginal likelihood is highly sensitive to its specification. Determining a suitable value for  $g$  has been extensively debated in the literature. The most common choice is letting  $g = n$ , referred to as the unit information prior ([Kass and Wasserman, 1995](#)). This idea has also been widely adopted in the literature on nonparametric regression using BMS (e.g. [Gustafson, 2000](#); [DiMatteo et al., 2001](#); [Kohn et al., 2001](#)). From the Bayesian perspective, the unit information prior can be viewed as a point mass prior at  $g = n$ , that is,  $\Pi(g) = \delta_n(g)$  with the Dirac measure  $\delta_b$  at  $b$ . Nevertheless, studies have reported that putting a suitable prior distribution on  $g$ , known as mixtures of g-priors, leads to improved empirical performance while addressing the paradoxes in BMS ([Liang et al., 2008](#); [Li and Clyde, 2018](#)). To unify various mixtures of g-priors, we use a broad family that encompasses various mixture distributions. Specifically, following [Li and Clyde \(2018\)](#), we assign the truncated compound confluent hypergeometric (tCCH) distribution to  $(g+1)^{-1}$  ([Gordy, 1998b](#)), that is,

$$\frac{1}{g+1} \sim \text{tCCH}\left(\frac{a}{2}, \frac{b}{2}, r, \frac{s}{2}, \nu, \kappa\right), \quad a, b, \kappa > 0, \quad r, s \in \mathbb{R}, \quad \nu \geq 1. \quad (10)$$

The tCCH distribution is a type of generalized beta distributions with five parameters that allow for a multi-modal or long-tailed density. The parameters  $a$  and  $b$  exhibit behavior akin to those of a beta distribution. The parameters  $r$ ,  $s$ , and  $\kappa$  govern the skewness of the density, while the parameter  $\nu$  determines the support. Further discussions, including the density and moments, of the tCCH distribution are presented in Section S1 of the supplementary material.

Table 1 shows a few distributions belonging to the tCCH family: the uniform prior (on  $(g+1)^{-1}$ ), the hyper-g and hyper-g/n priors ([Liang et al., 2008](#)), beta-prime prior ([Maruyama](#)

	$a$	$b$	$r$	$s$	$\nu$	$\kappa$	Concentration
Uniform	2	2	0	0	1	1	$g = O(1)$
Hyper-g	1	2	0	0	1	1	$g = O(1)$
Hyper-g/n	1	2	1.5	0	1	$n^{-1}$	$g = O(n)$
Beta-prime	0.5	$n - J_\xi - 1.5$	0	0	1	1	$g = O(n)$
ZS-adapted	1	2	0	$n + 3$	1	1	$g = O(n)$
Robust	1	2	1.5	0	$\frac{n+1}{J_\xi+1}$	1	$g = O(n)$
Intrinsic	1	1	1	0	$\frac{n+J_\xi+1}{J_\xi+1}$	$\frac{n+J_\xi+1}{n}$	$g = O(n)$

Table 1: Distributions belonging to the tCCH family.

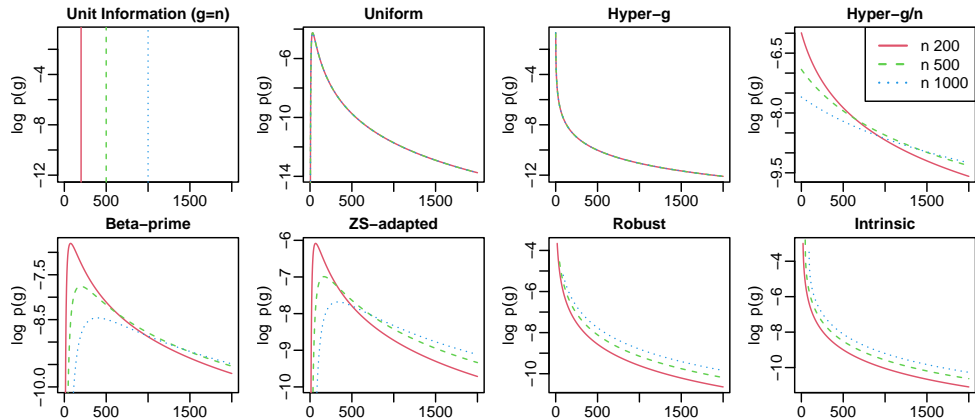


Figure 1: Distributions belonging to the tCCH family for  $n = 200, 500, 1000$ , with  $J_\xi = 10$  if required.

and George, 2011), Zellner Siow (ZS)-adapted prior (Held et al., 2015), robust prior (Bayarri et al., 2012), and intrinsic prior (Womack et al., 2014). The beta-prime prior is proper only if  $J_\xi < n - 1$ , so this restriction needs to be incorporated in  $\Pi(\xi)$  if the beta-prime prior is used. According to Li and Clyde (2018), the prior distributions are classified into two groups based to the prior concentration:  $g = O(1)$  and  $g = O(n)$ . (Notation can be misleading; it refers to the order of concentration of the distribution rather than the value of  $g$ . Maruyama and George (2011) also uses the same notation.) Figure 1 illustrates how the concentration of each prior distribution on  $g$  behaves.

Defining the confluent hypergeometric function of two variables (Gordy, 1998b) as  $\Phi_1(\alpha, \beta, \gamma, x, y) = B(\alpha, \gamma - \alpha)^{-1} \int_0^1 u^{\alpha-1} (1-u)^{\gamma-\alpha-1} (1-yu)^{-\beta} e^{xu} du$ , for  $\gamma > \alpha > 0$ ,  $\beta > 0$ ,  $x \in \mathbb{R}$ , and  $y < 1$ ,<sup>2</sup> the resulting marginal likelihood is expressed as

$$p(Y \mid \xi) = p(Y \mid \hat{\eta}_\xi) \text{tr}(J_n(\hat{\eta}_\xi))^{-1/2} \nu^{-J_\xi/2} \exp\left(-\frac{Q_\xi}{2\nu}\right) \frac{B((a + J_\xi)/2, b/2)}{B(a/2, b/2)} \times \Phi_1\left(\frac{b}{2}, r, \frac{a + b + J_\xi}{2}, \frac{s + Q_\xi}{2\nu}, 1 - \kappa\right) / \Phi_1\left(\frac{b}{2}, r, \frac{a + b}{2}, \frac{s}{2\nu}, 1 - \kappa\right), \quad (11)$$

<sup>2</sup>These parameter ranges ensure that  $\Phi_1$  is finite, positive, and real; see Theorem 1 of Gordy (1998b).

where  $B(\cdot, \cdot)$  is the beta function. The derivation of (11) can be found in Section S3 of the supplementary material. Generally, the evaluation of  $\Phi_1$  cannot be analytically performed and has to rely on numerical approximation. To calculate  $\Phi_1$ , we use the Gaussian-Kronrod quadrature routine available in the Boost C++ library.

The approximate posterior for  $((g+1)^{-1}, \alpha, \beta_\xi)$  conditional on  $\xi$  is given by

$$\begin{aligned} \frac{1}{g+1} \mid Y, \xi &\sim \text{tCCH}\left(\frac{a+J_\xi}{2}, \frac{b}{2}, r, \frac{s+Q_\xi}{2}, \nu, \kappa\right), \\ \beta_\xi \mid Y, g, \xi &\sim N\left(\frac{g}{g+1}\hat{\beta}_\xi, \frac{g}{g+1}(\tilde{B}_\xi^T J(\hat{\eta}_\xi) \tilde{B}_\xi)^{-1}\right), \\ \alpha \mid Y, g, \beta_\xi, \xi &\sim N\left(\hat{\alpha}_\xi - \text{tr}(J_n(\hat{\eta}_\xi))^{-1} 1_n^T J_n(\hat{\eta}_\xi) B_\xi (\beta_\xi - \hat{\beta}_\xi), \text{tr}(J_n(\hat{\eta}_\xi))^{-1}\right). \end{aligned} \quad (12)$$

The derivation of (12) is provided in Section S3 of the supplementary material. The expression is also valid for the unit information prior by replacing the first line with the point mass posterior,  $\Pi(g \mid Y, \xi) = \delta_n(g)$ . Sampling from tCCH distributions can be conducted through MCMC, but exact sampling is available under certain prior specification. We observe that if any of the uniform prior, hyper-g prior, ZS-adapted prior, or robust prior is used, the first line of (12) is reduced to a truncated gamma distribution, and exact sampling is straightforward. For the remaining priors, slice sampling with data augmentation can be employed. Details on sampling are available in Section S4 of the supplementary material. The joint posterior  $\Pi(\alpha, \beta_\xi, \xi, g \mid Y)$  is fully specified by the posterior in (12) and the marginal posterior of  $\xi$ ,  $\Pi(\xi \mid Y)$ . The latter one is obtained by specifying a prior  $\Pi(\xi)$  as in Section 4 and deploying the expression for the approximate marginal likelihood  $p(Y \mid \xi)$  in (11) (or  $p(Y \mid g, \xi)$  in (9) for the unit information prior). The posterior distribution of a functional in (6) is then easily evaluated by directly marginalizing  $\xi$  out or using MCMC for Monte Carlo integration of  $\xi$ , depending on a prior for  $\xi$  specified in Section 4.

### 3.2 Behavior of the Bayes factor

The influence of  $g$  is crucial for achieving reasonable sparsity in model selection with the g-prior (Kass and Raftery, 1995). A large  $g$  favors sparse models, while a small  $g$  advocates complex models. Choosing a suitable  $g$  is particularly important in our additive model setup because it directly controls the smoothness of the additive functions. In the literature on nonparametric regression with basis expansion, many previous studies have relied on the unit information prior induced by the choice  $g = n$  (e.g. Gustafson, 2000; DiMatteo et al., 2001; Kohn et al., 2001). However, as previously mentioned, a mixture of g-priors leads to improved empirical performance in BMS (Liang et al., 2008; Li and Clyde, 2018). While attempts have been made to assign a prior on  $g$  for nonparametric regression (Jeong and Park, 2016; Jeong et al., 2017; Francom et al., 2018; Francom and Sansó, 2020; Jeong et al., 2022), there is a lack of a thorough investigation into the differences from the unit information prior. In this section, we examine how mixtures of g-priors behave in contrast to the unit information prior with  $g = n$  and discuss why the unit information prior may not be the best choice for estimating GAMs.

Our investigation relies on the Bayes factors. For two knots  $\xi_{(1)}$  and  $\xi_{(2)}$ , the Bayes factor of  $\xi_{(1)}$  to  $\xi_{(2)}$  is defined as  $BF[\xi_{(1)}; \xi_{(2)}] = p(Y \mid \xi_{(1)})/p(Y \mid \xi_{(2)})$ . For the exponential family models with known  $\phi$ , the marginal likelihood  $p(Y \mid \xi)$  is expressed by (9) with  $g = n$  for the unit

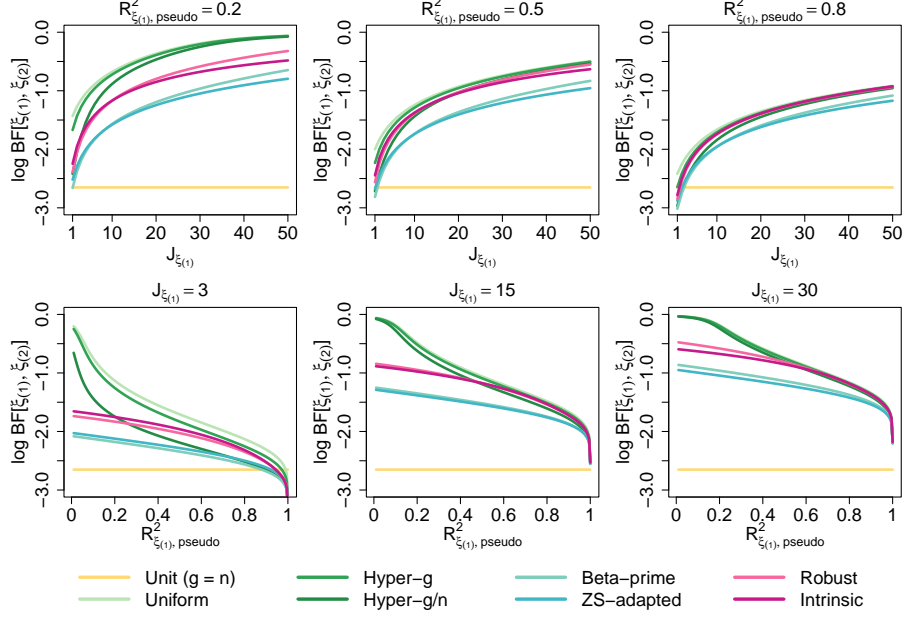


Figure 2: Change in  $\log BF[\xi_{(1)}; \xi_{(2)}]$  as a function of  $J_{\xi_{(1)}}$  ( $= J_{\xi_{(2)}} + 1$ ) and  $R_{\xi_{(1)}, \text{pseudo}}^2$  ( $= R_{\xi_{(2)}, \text{pseudo}}^2$ ) for  $n = 1000$ .

information prior and by (11) for mixtures of g-priors induced by the tCCH prior on  $(g+1)^{-1}$ . To understand how the Bayes factor penalizes model complexity, we consider two knots  $\xi_{(1)}$  and  $\xi_{(2)}$  such that  $J_{\xi_{(1)}} = J_{\xi_{(2)}} + 1$  and  $\hat{\eta}_{\xi_{(1)}} = \hat{\eta}_{\xi_{(2)}}$ . In other words, both knots contribute equally to model fit, but  $\xi_{(1)}$  has one more redundant knot-point than  $\xi_{(2)}$ . The Bayes factor  $BF[\xi_{(1)}; \xi_{(2)}]$  can be interpreted as a preference measure for the larger model with one more redundant knot-point over the smaller model. In essence, the larger the value of the Bayes factor, the stronger the preference for the larger model. We aim to observe the behavior of the Bayes factor as  $J_{\xi_{(1)}}$  and the goodness-of-fit change. In Gaussian regression, the goodness-of-fit can be naturally assessed by the coefficient of determination. For the exponential family models, the pseudo- $R^2$ , defined as  $1 - \exp(-D/n)$  with the usual deviance statistic  $D$ , can be used alternatively (Cox and Snell, 1989; Magee, 1990), with the caveat that its maximum value may be less than 1 depending on the specific model (Nagelkerke, 1991). To represent the Bayes factor as a function of the pseudo- $R^2$ , we use the fact that  $Q_\xi$  is asymptotically equivalent to the deviance  $D$  under mild conditions (Held et al., 2015; Li and Clyde, 2018). Therefore, we define  $R_{\xi, \text{pseudo}}^2 = 1 - \exp(-Q_\xi/n)$  to gauge the goodness-of-fit in the exponential family models.

Figure 2 visualizes a toy example with  $n = 1000$ , which shows how  $\log BF[\xi_{(1)}; \xi_{(2)}]$  changes with  $J_{\xi_{(1)}}$  (which equals  $J_{\xi_{(2)}} + 1$ ) and  $R_{\xi_{(1)}, \text{pseudo}}^2$  (which equals  $R_{\xi_{(2)}, \text{pseudo}}^2$ ). The unit information prior consistently produces a constant Bayes factor regardless of  $J_{\xi_{(1)}}$  and goodness-of-fit. In contrast, the first row of Figure 2 shows that the preference for the larger model, indicated by the mixture priors, increases with the model size  $J_{\xi_{(1)}}$ . This implies that, when comparing small models, mixtures of g-priors tend to favor the smaller model ( $\xi_{(2)}$ ) unless there is a significant improvement in the marginal likelihood. Conversely, when comparing large models, mixture priors may advocate for the larger one ( $\xi_{(1)}$ ), even without a clear gain. This property can be useful in

improving GAM estimation performance because, with basis expansion generally yielding large models, we aim to detect local and global signals of the target functions that may be easily missed. The second row of Figure 2 illustrates that the preference for the larger model induced by the mixture priors weakens as the goodness-of-fit measurement increases. This aligns with intuition, as with a sufficiently high goodness-of-fit, choosing the more complex model might not be desirable, and opting for the simpler one is preferable, unless the complex model brings about a significant improvement in the marginal likelihood. The unit information prior ignores such characteristics in GAM estimation.

Figure 2 also demonstrates the differences among the mixtures of g-priors. The beta-prime and ZS-adapted priors behave similarly and exhibit the weakest inclination for the larger model. The robust and intrinsic priors show comparable decays to each other and exhibit a stronger preference for the larger model compared to the beta-prime and ZS-adapted priors. The two  $O(1)$ -type priors (uniform and hyper-g) express a more pronounced preference for the larger model than the  $O(n)$ -type priors. Notably, the hyper-g/n prior, though belonging to the  $O(n)$  family, appears somewhat akin to the  $O(1)$ -type priors. When  $R_{\xi_{(1)},\text{pseudo}}^2$  is small, these later three priors drive  $\log BF[\xi_{(1)}; \xi_{(2)}]$  close to zero. This implies that when the null model is true, and hence  $R_{\xi_{(1)},\text{pseudo}}^2$  is close to zero, the preferences for the smaller and larger models become similar, potentially leading to overfitting. While the figure suggests that other mixture priors seem relatively unaffected by this issue, it remains unclear which mixture prior performs best for GAMs. Our numerical studies in Section 5 indicate that the robust and intrinsic priors are the most suitable. The following proposition provides a basic interpretation of where the differences among the mixtures of g-priors may arise.

**Proposition 3.** *For the model in (1) and (2) with the priors in (7) and (8), consider two knots  $\xi_{(1)}$  and  $\xi_{(2)}$  such that  $J_{\xi_{(1)}} = J_{\xi_{(2)}} + k$  and  $\hat{\eta}_{\xi_{(1)}} = \hat{\eta}_{\xi_{(2)}}$ , where  $k$  is a positive integer. Then, for any positive integer  $k$ ,*

$$BF[\xi_{(1)}; \xi_{(2)}] = \begin{cases} (1+b)^{-k/2}, & \text{if } g \sim \delta_b, \\ E[(1+g)^{-k/2} \mid \xi_{(2)}, Y], & \text{if } g \sim tCCH(a/2, b/2, r, s/2, \nu, \kappa). \end{cases}$$

A proof can be found in Section S2 of the supplementary material. This proposition implies that the Bayes factor  $BF[\xi_{(1)}; \xi_{(2)}]$  is the conditional posterior mean of  $(1+g)^{-k/2}$  induced by the unit information prior or tCCH prior. In this respect, the proposition explicitly shows why the Bayes factor induced by the unit information prior is constant. The differences in the Bayes factors induced by the mixture priors can be attributed to different posterior means of the shrinkage factor  $(1+g)^{-k/2}$ .

As a final note, in conjunction with a specified prior for knots  $\Pi(\xi)$ , the actual model comparison for determining basis terms relies on the posterior odds  $\Pi(\xi_{(1)} \mid Y)/\Pi(\xi_{(2)} \mid Y)$  rather than the Bayes factor. Instead of employing the mixtures of g-priors, one may consider adjusting the posterior odds induced by the unit information prior using a suitable prior for knots  $\Pi(\xi)$ . While not entirely impossible, we view this as an unfavorable approach because a prior for knots must be highly data-dependent for the posterior odds, with the unit information prior distribution, to vary with the goodness-of-fit measurement. Using the mixtures of g-priors with a usual prior for knots is a more natural choice.

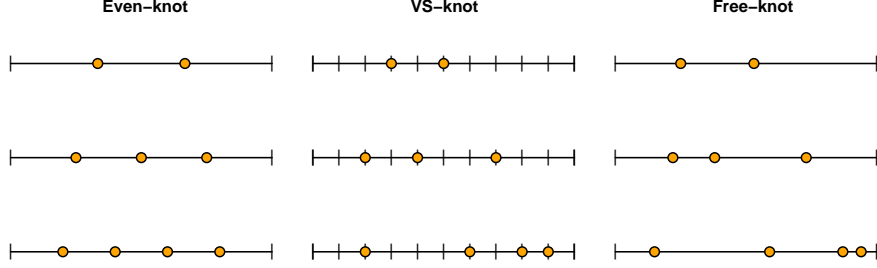


Figure 3: A graphical illustration of the three strategies for constructing  $\Xi$  discussed in Sections 4.1–4.3. For the even-knot splines, the locations of knots are deterministically ascertained once  $|\xi_j|$  is chosen. The VS-knot splines select knot-points from a pre-determined set of locations. The free-knot splines are the most flexible and have no such limitation.

## 4 Priors for knots

A prior  $\Pi(\alpha, \beta_\xi \mid \xi)$  on the coefficients was specified in Section 3. To complete the Bayesian framework, we consider a few different options for specifying  $\Pi(\xi)$  for knots. Our prior for  $\beta_\xi$  requires  $B_\xi$  to be of full-column rank (see (8) above). Therefore, we choose  $\Pi(\xi)$  with the condition that  $B_\xi$  is of full-column rank with prior probability one, that is,  $\Pi(\text{rk}(B_\xi) = J_\xi) = 1$ . This is often fulfilled by the restriction  $J_\xi < n$  if the knots and design points are well-distributed.

Intuitively,  $\xi_j$  can consist of any singletons lying on the interval  $(\xi_j^L, \xi_j^U)$ , indicating that the intrinsic parameter space for  $\xi_j$  is infinite-dimensional. However, finite truncation to restricted support may be helpful for computational reasons. As mentioned earlier, we denote  $\Xi$  as the induced support of  $\Pi(\xi)$ . The support  $\Xi$  restricts the function class generated by our natural cubic spline basis terms. A smaller space reduces model complexity but may fail to capture local and global features of the target function. This means that the restricted support  $\Xi$  balances estimation quality and computational efficiency, and is crucial to choose a prior with suitable  $\Xi$ . There have been various ideas of specifying  $\Xi$  for  $\Pi(\xi)$ . In this section, we gather the existing strategies for constructing  $\Xi$  that have been widely accepted in the literature and classify them into three categories. The three approaches are described in detail in Sections 4.1–4.3. Figure 3 provides a graphical summary of the strategies. A comparison among the empirical performances of the three approaches is performed in Section 5 based on a numerical study.

### 4.1 Even-knot splines: equidistant knots

The simplest but powerful Bayesian adaptation arises from the assumption that the number of knots is not fixed but their locations are determined by an intrinsic law. The idea has been extensively considered in the literature and has been empirically and theoretically successful (e.g., [Rivoirard and Rousseau, 2012](#); [De Jonge and Van Zanten, 2012](#); [Shen and Ghosal, 2015](#)). We refer to this approach as the *even-knot splines*. The name should be carefully understood because evenness may be assessed by the empirical measure rather than a geometric distance.

Specifically, a prior is assigned on the number  $|\xi_j|$  of knots  $\xi_j$  for  $j = 1, \dots, p$ . The remaining specification on  $\xi$  is automatically completed by a given rule. For example, with a given number

$|\xi_j|$ , the knots  $\xi_j$  may be equally spaced or chosen based on the quantiles of  $\tilde{X}_j$ , where  $\tilde{X}_j$  is the set of unique values of the design points  $x_{ij}, i = 1, \dots, n$ . We prefer the latter for a stable implementation. Using the quantiles also ensures full-column rank of  $B_\xi$  as soon as  $J_\xi < n$ , if there are no duplicates in  $x_{ij}, i = 1, \dots, n$ . For computational reasons, it is useful to put a cap on each  $|\xi_j|$  such that  $|\xi_j| \leq M_j$  for a predetermined  $M_j$ . The induced support is defined as

$$\Xi_{EK} = \left\{ \xi : \text{rk}(B_\xi) = J_\xi, |\xi_j| \leq M_j, \xi_{jk} = Q_j \left( \frac{k}{|\xi_j| + 1} \right), j = 1, \dots, p, k = 1, \dots, |\xi_j| \right\},$$

where  $Q_j$  is the quantile function of  $\tilde{X}_j$ , for  $j = 1, \dots, p$ . Examples of knots belonging to  $\Xi_{EK}$  are illustrated in Figure 3. With an unnormalized density  $q_j : \{0, 1, \dots, M_j\} \rightarrow (0, \infty)$  on  $|\xi_j|$ , the prior can be formally expressed as

$$\pi_{EK}(\xi) \propto \mathbb{1}\{\text{rk}(B_\xi) = J_\xi\} \prod_{j=1}^p q_j(|\xi_j|). \quad (13)$$

Further discussion on the density  $q_j$  is provided in Section 4.4.

The key benefit of the prior in (13) is that it has low model complexity; that is, we can enumerate all possible models for moderately large  $p$  because  $|\Xi_{EK}| \leq \prod_{j=1}^p (1 + M_j)$ . This enables MCMC-free posterior computation for relatively low-dimensional problems. If  $p$  is too large to list all possibilities, the Metropolis-Hastings algorithm can be useful for exploring the model spaces with a proposal that increases or decreases  $|\xi_j|$  at a time. In this situation, computation may be facilitated by saving the value of the marginal likelihood  $p(Y | \xi)$  with current  $\xi$  and utilizing it whenever the same  $\xi$  is revisited. We observe that the storing idea works well unless  $p$  is extremely large.

Although the even-knot splines approach substantially reduces the model complexity, its major downside arises from its deterministic rule. Specifically, owing to the nature of construction, it is impossible to deal with functions with spatially adaptive smoothness such as a Doppler function. This drawback motivates the need for more flexible constructions discussed in the next two subsections.

## 4.2 VS-knot splines: knot selection

The limitation of the even-knot splines in Section 4.1 can be relaxed by considering a prior inducing a richer  $\Xi$  that allows for spatial adaptation. This can be fulfilled by allowing knot placement as well as the number of knots to be data-driven. A common strategy is setting a large set of basis functions and choosing important ones among the candidates using Bayesian variable selection. The idea was initiated by [Smith and Kohn \(1996\)](#) and has been widely used in the literature on nonparametric regression (e.g., [Kohn et al., 2001](#); [Chan et al., 2006](#); [Jeong and Park, 2016](#); [Jeong et al., 2017](#); [Park and Jeong, 2018](#); [Jeong et al., 2022](#)). Given that the approach is based on variable selection, we refer to it as the *VS-knot splines*.

Consider a set  $\xi_j^c = \{\xi_{j1}^c, \dots, \xi_{jM_j}^c\}$  of knot candidates such that  $\xi_j^L < \xi_{j1}^c < \dots < \xi_{jM_j}^c < \xi_j^U$  with large enough  $M_j < n$ . Similar to Section 4.1,  $\xi_j^c$  can be equidistant or determined by the sample quantiles of  $\tilde{X}_j$ . We prefer the latter setup for the same reason. The actual knots  $\xi_j$  are

chosen as a subset of  $\xi_j^c$  (including an empty set) using BMS. Accordingly, the support consists of all possible subsets of  $\{\xi_1^c, \dots, \xi_p^c\}$  with the restriction  $\text{rk}(B_\xi) = J_\xi$ , that is,

$$\Xi_{VS} = \{\xi : \text{rk}(B_\xi) = J_\xi, \xi_j \subset \xi_j^c, j = 1, \dots, p\}.$$

Similar to Section 4.1, we assign an unnormalized density  $q_j : \{0, 1, \dots, M_j\} \rightarrow (0, \infty)$  to  $|\xi_j|$ . We then assign equal weights to all knot locations conditional on  $|\xi_j|$ . The resulting prior is given by

$$\pi_{VS}(\xi) \propto \mathbb{1}\{\text{rk}(B_\xi) = J_\xi\} \prod_{j=1}^p q_j(|\xi_j|) \binom{M_j}{|\xi_j|}^{-1}. \quad (14)$$

The prior has been shown to be successful in adapting to spatially inhomogeneous smoothness (e.g., [Chan et al., 2006](#); [Jeong and Park, 2016](#); [Jeong et al., 2017](#)). The cardinality  $|\Xi_{VS}| \leq 2^{\sum_{j=1}^p M_j}$  shows that it is usually impractical to enumerate all possible models, indicating that MCMC is useful for exploring the model spaces. The standard Gibbs sampling and Metropolis-Hastings algorithm can be easily applied to this setup ([Dellaportas et al., 2002](#)). Sampling efficiency may be improved by block updates ([Kohn et al., 2001](#); [Jeong et al., 2022](#)) or adaptive sampling ([Nott and Kohn, 2005](#); [Ji and Schmidler, 2013](#)). Moreover, as  $\Xi_{VS}$  is finite-dimensional, the idea of storing the marginal likelihood discussed in Section 4.1 seems viable. However, our experience shows that this approach is effective only when  $p$  is very small because of the memory issue, for example,  $p \leq 2$ . Thus, we do not pursue this direction.

We emphasize that our basis system in (5) is particularly useful for the VS-spline approach. Given Proposition 2, knot selection is naturally translated into basis selection with the linear term  $b_{j1}^*$  always being included. This property simplifies computation using the basis system the basis system in (4) and (5); one can generate a full basis matrix  $B_j^c \in \mathbb{R}^{n \times (M_j+1)}$  whose  $(i, k)$ th component is  $b_{jk}(x_{ij})$  constructed with the knot candidates  $\xi_j^c = (\xi_{j1}^c, \dots, \xi_{jM_j}^c)$ , and then choose important columns of  $B_j^c$ , while always including the first column for the linear term. As noted previously, this approach is not attainable with other natural cubic spline basis functions, such as the natural cubic B-splines or the ones in (5.4) and (5.5) of [Hastie et al. \(2009\)](#). For these basis functions, a basis term  $b_{j,k+1}^*$  is potentially specified with more than one knot-point for some  $k$ . Therefore, inserting or deleting a knot-point may alter more than one basis term, leading to a conflict between knot selection and basis selection.

### 4.3 Free-knot splines

The strategy of the VS-splines in Section 4.2 chooses important knot locations among a set of predetermined candidates. The resulting knots are not equally spaced so that they can account for spatially varying degree of smoothness. Despite this flexibility, there is a further desire to relax the restriction coming from the discrete set of knot candidates, with a fully nonparametric setup by allowing knots to be any singletons in the given range as soon as the induced  $B_\xi$  is of full-column rank. The idea is referred to as the *free-knot splines* ([Denison et al., 1998](#); [DiMatteo et al., 2001](#)).

Similar to Section 4.1, it can be useful to put a cap on each  $|\xi_j|$  such that  $|\xi_j| \leq M_j$  for a predetermined  $M_j$ . The resulting support for  $\xi$  is

$$\Xi_{FK} = \left\{ \xi : \text{rk}(B_\xi) = J_\xi, |\xi_j| \leq M_j, \xi_j^L < \xi_{j1} < \dots < \xi_{j|\xi_j|} < \xi_j^U, j = 1, \dots, p \right\}.$$

It is clear that  $\Xi_{FK}$  is uncountable. The prior is specified in a manner similar to (14). However, as the map  $|\xi_j| \mapsto \xi_j$  is a surjection and not a bijection, a conditional prior density of  $\xi_j$  given  $|\xi_j|$ , denoted by  $\tilde{q}_j(\cdot \mid |\xi_j|)$ , should be specified on the corresponding support. Following DiMatteo et al. (2001), we choose  $\tilde{q}_j$  induced by the uniform prior on the  $|\xi_j|$ -simplex by scaling  $(\xi_j^L, \xi_j^U)$  to  $(0, 1)$ . With an unnormalized density  $q_j : \{0, 1, \dots, M_j\} \rightarrow (0, \infty)$ , the prior on  $\xi_j$  is formalized as

$$\pi_{FK}(\xi) \propto \mathbb{1}\{\text{rk}(B_\xi) = J_\xi\} \prod_{j=1}^p q_j(|\xi_j|) \tilde{q}_j(\xi_j \mid |\xi_j|). \quad (15)$$

Our free-knot spline prior in (15) is slightly more general than the original construction by DiMatteo et al. (2001) because at least one knot must be included in their construction, whereas we relaxed such limitation to account for a completely linear effect using an empty knot. The posterior distribution can be explored by the reversible jump MCMC with birth, death, and relocation proposals (DiMatteo et al., 2001). Thus, the computation is generally more demanding than the VS-knot splines. The advantage is that the prior is inherently more flexible than the one in (14) and has a better ability to approximate the target functions. However, our experience shows that there is no significant improvement observed in the free-knot splines in most practical examples. Given that the reversible jump MCMC is often inefficient, this fact underscores the importance of avoiding the inadvertent use of the free-knot splines. Our simulation study in Section 5 reveals that, while the performance measures for the free-knot splines are comparable with those for the VS-knot splines, the sampling efficiency (measured as the ratio of the effective sample size and runtime) of the free-knot splines is significantly lower.

Similar to the VS-knot splines approach, the basis construction in (4) and (5) is useful for the free-knot splines. According to Proposition 2, adding or removing a knot-point corresponds to adding or removing the corresponding basis term. Therefore, the reversible jump MCMC can be conducted by adding or removing a column of the matrix, without the need to reconstruct the entire basis terms.

#### 4.4 Prior distribution on $|\xi_j|$

The priors described in Sections 4.1–4.3 require specifying the unnormalized density  $q_j$  for  $|\xi_j|$ . To achieve the desired optimal properties in nonparametric regression, previous studies indicate that priors for the BMS-based methods must exhibit suitably decaying tail properties (e.g, Shen and Ghosal, 2015). Priors with guaranteed tail properties include Poisson and geometric distributions (with a suitable truncation if required by the setup). However, determining a practically suitable prior decay remains uncertain. In the literature on variable selection, another common choice, believed to be weakly informative, is a discrete uniform distribution on  $\{0, 1, \dots, M_j\}$ , resulting in the so-called hierarchical uniform prior on  $\xi_j$  (Kohn et al., 2001; Cripps et al., 2005; Scott and Berger, 2010). To balance the theoretical appeal in nonparametric regression with practical model selection considerations, our default prior is set to be a truncated geometric distribution with a small success probability  $\varpi$ . Specifically, the unnormalized density is given by

$$q_j(u) = (1 - \varpi)^u \varpi, \quad u = 0, 1, \dots, M_j. \quad (16)$$

By choosing a value close to zero for  $\varpi$ , the prior in (16) closely resembles the discrete uniform distribution, while preserving the desired tail property for optimality. However, we observed that using a reasonably small value for  $\varpi$  enhances stability in estimating knot specification. Therefore, we adopt  $\varpi = 0.1$  as our default value.

The unnormalized density  $q_j$  is also applicable in GAPLMs, where a few predictor variables are assumed to have linear effect (e.g., binary variables). This is achieved by fixing specific  $f_j$  to include only the linear basis term  $N_1$ . Accordingly, If some predictor variables have a linear effect, we set  $q_j$  to have a point mass at zero for such  $j$ , that is,  $\Pi(|\xi_j| = 0) = 1$ , and use the prior in (16) for nonparametric additive components.

## 5 Numerical study

The primary goal of this study is to explore the behavior of the mixtures of g-priors in the BMS-based approaches for estimating GAMs. While Section 3.2 offers foundational insights, the most suitable mixture prior for GAMs remains uncertain. Additionally, we aim to assess the three approaches for specifying priors for knots, as discussed in Section 4, and compare them with other Bayesian methods for function estimation, such as Bayesian P-splines. This section presents a simulation study designed to achieve these objectives.

### 5.1 Comparison among the mixtures of g-priors

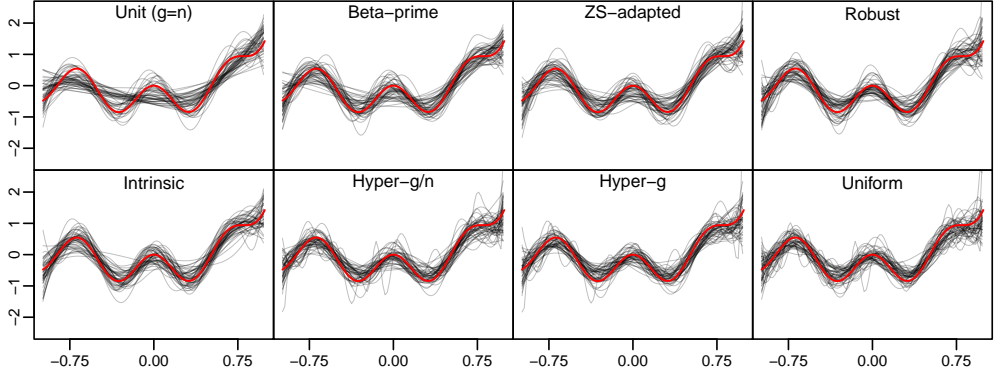
We first conduct a simulation study that reveals the differences among the performances of the mixtures of g-priors for estimation of GAMs. Regarding the synthetic functions, we consider the following three uncentered functions  $f_j^* : [-1, 1] \rightarrow \mathbb{R}$ ,  $j = 1, 2, 3$ :

$$\begin{aligned} f_1^*(x) &= 0.5(2x^5 + 3x^2 + \cos(3\pi x) - 1), \\ f_2^*(x) &= \frac{21(3x + 1.5)^3}{8000} + \frac{21(3x - 2.5)^2}{400e^{-3x-1.5}} \sin\left(\frac{(3x + 1.5)^2\pi}{3.2}\right) \mathbb{1}\{-0.5 < x < 0.85\}, \\ f_3^*(x) &= x. \end{aligned} \quad (17)$$

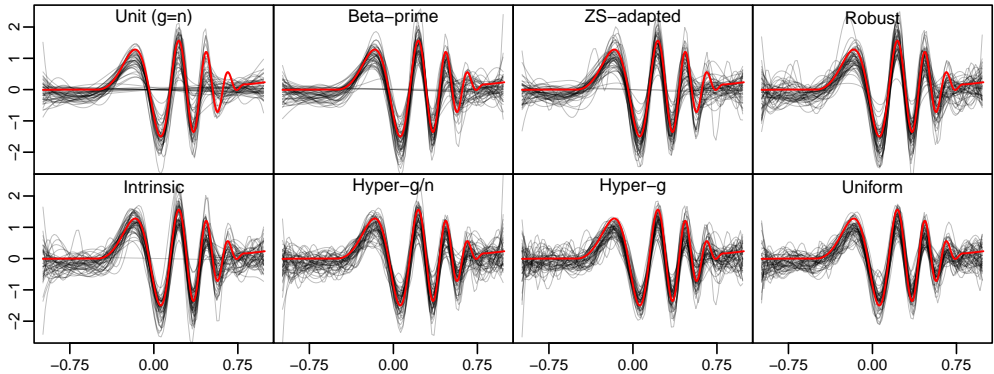
Specifically,  $f_1^*$  is a nonlinear function that is not a polynomial,  $f_2^*$  is a nonlinear function with locally varying smoothness, and  $f_3^*$  is a linear function. The two nonlinear functions  $f_1^*$  and  $f_2^*$  are modified from [Gressani and Lambert \(2021\)](#) and [Francom and Sansó \(2020\)](#), respectively. The functions are visualized in Figure 4 with suitable centering.

The simulation datasets are generated by the exponential family model with the additive predictor  $\eta_i = \sum_{j=1}^3 f_j^*(x_{ij}) = \alpha + \sum_{j=1}^3 f_j(x_{ij})$ , where  $x_{ij}$  are drawn independently from  $\text{Unif}(-1, 1)$ ,  $f_j$  is the centered version of  $f_j^*$  and  $\alpha$  is the induced intercept. In this section, we present simulation results for a nonlinear logistic regression model given by  $Y_i \sim \text{Bernoulli}(e^{\eta_i}/(1 + e^{\eta_i}))$ . Section S6 of the supplementary material includes a simulation study for Poisson regression  $Y_i \sim \text{Poi}(e^{\eta_i})$  and Gaussian regression  $Y_i \sim N(\eta_i, \sigma^2)$ .

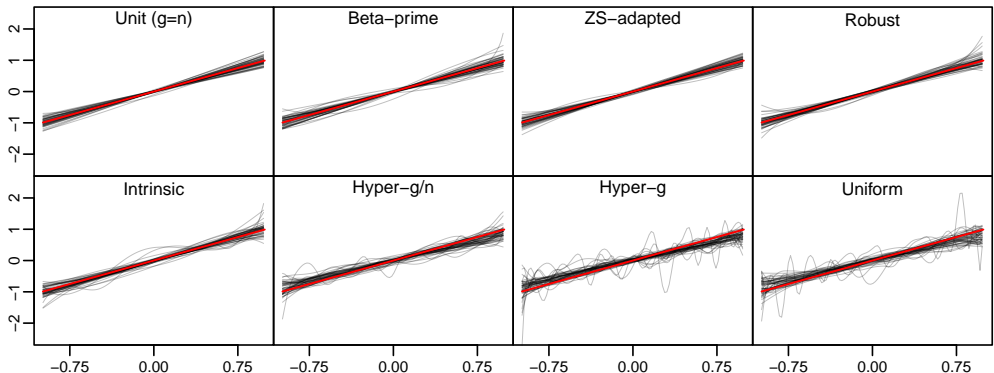
In Section 5.2, we will observe that the VS-knot splines approach works reasonably well among the three strategies for choosing  $\Xi$  described in Section 4. Accordingly, we specifically focus on the VS-knot splines in this section. For each of the logistic regression models with  $n = 500, 1000, 2000$ , we generate 500 replications of datasets and estimate  $f_j$  using the VS-knot splines comprising 30



(a) Pointwise posterior mean estimates of  $f_1$  in 50 replications



(b) Pointwise posterior mean estimates of  $f_2$  in 50 replications



(c) Pointwise posterior mean estimates of  $f_3$  in 50 replications

Figure 4: Pointwise posterior means (gray) of  $f_1$ ,  $f_2$ , and  $f_3$  in the nonparametric logistic regression model with  $n = 1000$ , obtained from randomly chosen 50 replicated datasets, along with the true function (red).

knot candidates with the unit information prior and the mixture priors summarized in Table 1, coupled with the truncated geometric prior with  $\varpi = 0.1$  on  $\xi_j$ . With each prior distribution, we obtain a Markov chain of length 10,000 to explore the posterior distribution until convergence after a suitable burn-in period. We calculate the root mean squared error (RMSE) and the

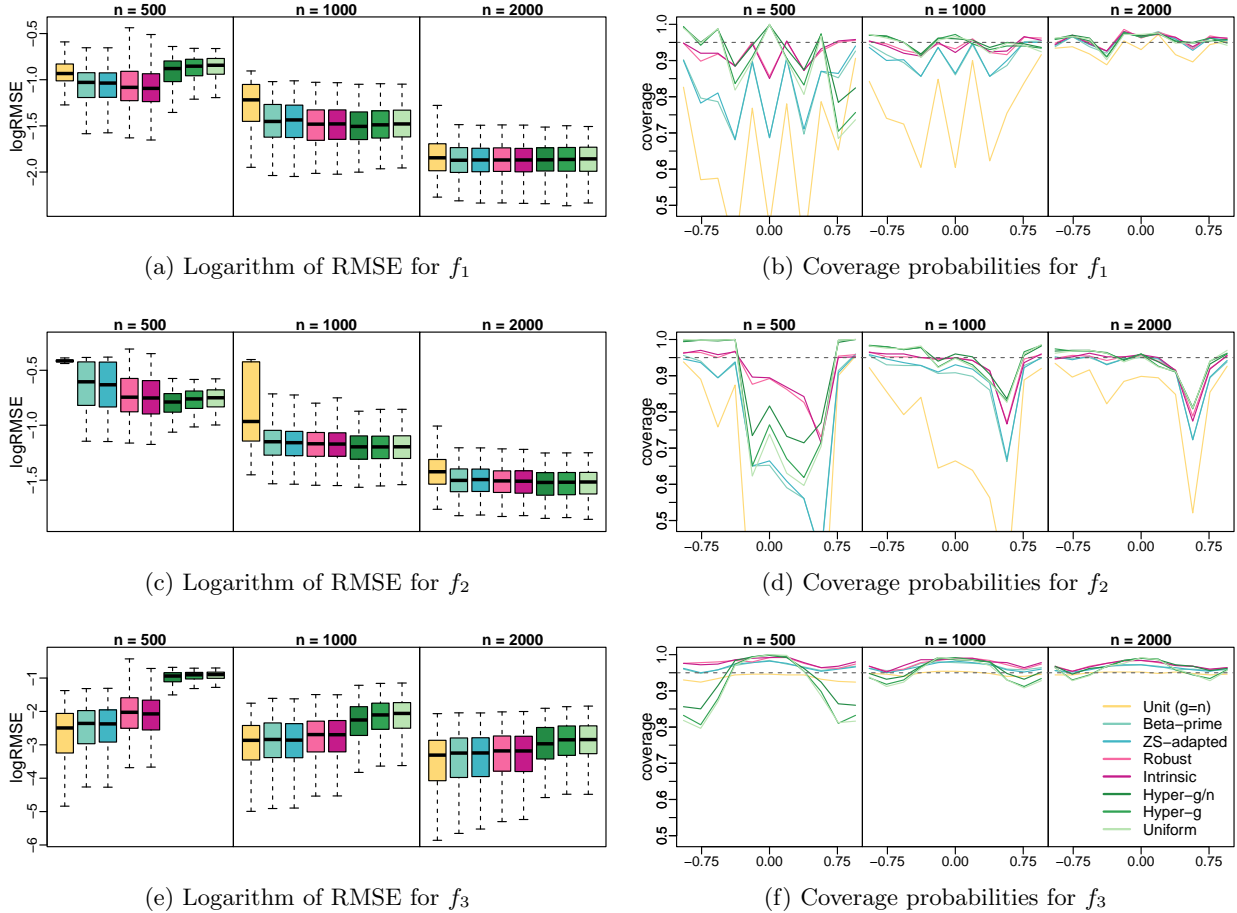


Figure 5: Logarithm of RMSE and coverage probabilities for  $f_1$ ,  $f_2$ , and  $f_3$  in the nonparametric logistic regression models with  $n = 500, 1000, 2000$ , obtained from 500 replicated datasets.

coverage probabilities of the 95% pointwise credible bands at a few given points.

Figures 4 and 5 summarize the simulation results. As discussed in Section 3.2, the unit information prior behaves markedly differently from the mixture priors; it generally underperforms for nonlinear function estimation and exhibits clear signs of underfitting. This suggests that the conventional use of the unit information prior for function estimation may be inappropriate. The primary challenge lies in determining which mixture prior is most suited for function estimation. Based on our simulation analysis, we conclude that the intrinsic and robust priors are the most suitable choices. Although the difference between the mixtures of g-priors is less distinct for a large sample size, it is evident that the intrinsic and robust priors consistently outperform the other priors across finite samples. The beta-prime and ZS-adapted priors tend to exhibit slight underfitting, whereas the uniform, hyper-g, and hyper-g/n priors tend to demonstrate overfitting. The latter observation aligns with our expectations discussed in Section 3.2. Across all functions, the robust and intrinsic priors achieve moderate RMSE and coverage properties, with the intrinsic prior being slightly more accurate in smaller samples. The simulation results for Poisson and Gaussian regression in the supplementary material also support a similar conclusion.

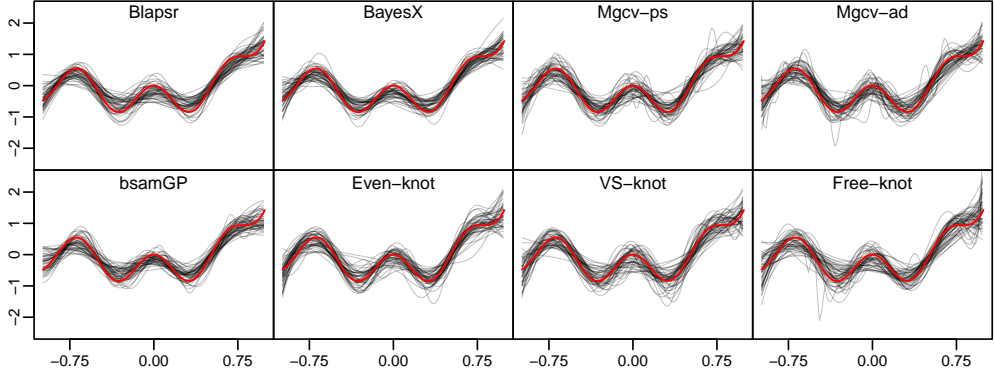
We recommend the intrinsic or robust prior as the default choice for a hierarchy of  $g$ .

## 5.2 Comparison with other methods

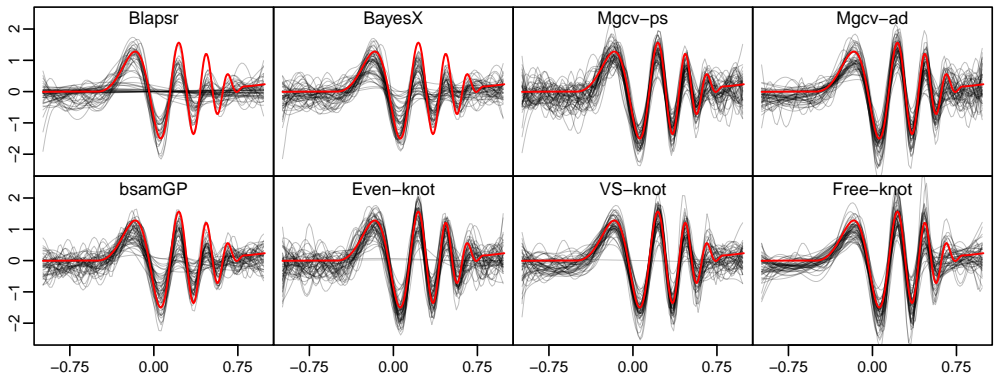
Now, we compare the BMS-based methods for GAMs with other Bayesian methods for function estimation. We consider the three strategies described in Section 4: the even-knot splines, VS-knot splines, and free-knot splines, along with a few competitors available in R packages: `R2BayesX` (Umlauf et al., 2015), `Blapsr` (Gressani and Lambert, 2021), `mgcv` (Wood, 2017), and `bsamGP` (Jo et al., 2019). In accordance with the results in Section 5.1, the three BMS-based approaches are equipped with the intrinsic prior. Notably, among the competitors, `mgcv` is the only frequentist method, while all other approaches are within the Bayesian framework. The methods `R2BayesX` and `Blapsr` are based on the Bayesian P-splines (Lang and Brezger, 2004). While `R2BayesX` offers conventional MCMC estimates, `Blapsr` provides the option to employ the Laplace approximation, particularly beneficial for a small number of additive components to enhance computational efficiency. In contrast, `bsamGP` utilizes the second-order Gaussian process to estimate nonparametric functions in GAMs.

The simulation specifications are carefully chosen to ensure a fair comparison among the methods. For the BMS-based approaches (i.e., the even-knot, VS-knot, and free-knot splines), the maximum number of knots  $M_j$  is consistently set to 30 for every  $j = 1, 2, 3$ . Likewise, we maintain  $M_j = 30$  for competitors relying on penalized splines (i.e., `R2BayesX`, `Blapsr`, and `mgcv`), ensuring that both the BMS-based and penalized spline approaches have comparable least penalized models. The `mgcv` package offers an option for locally adaptive estimation of smooth functions. We explore both the original version with a single smoothness parameter and a variant with local adaptation, denoted as `mgcv-ps` and `mgcv-ad` in the figures, respectively. As for `bsamGP`, we configure the number of cosine basis functions in the spectral representation of Gaussian process priors for each  $f_j$  to be identical to  $M_j$ . The simulation settings remain consistent with those in Section 5.1, using the functions specified in (17). In this section, we provide the simulation results for nonparametric logistic regression, while the results for Poisson and Gaussian regression can be found in Section S6 of the supplementary material. For each Bayesian method relying on MCMC, we obtain a Markov chain of length 10,000 explore the posterior distribution until achieving convergence after a suitable burn-in period. We calculate the RMSE and 95% pointwise credible bands at a few given points for each method. Here, we only present the results for logistic nonparametric regression. Additional results for Poisson and Gaussian regression are available in the supplementary material.

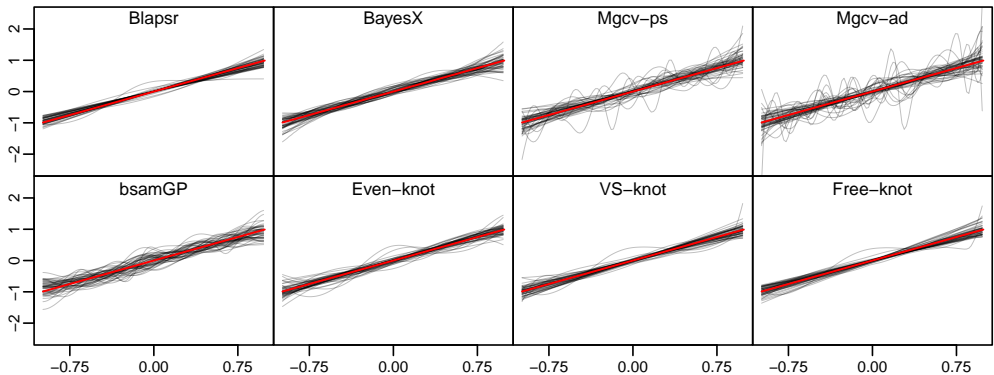
Figures 6 and 7 summarize the simulation results for the nonlinear logistic regression models. Upon observation, it is apparent that `R2BayesX` and `Blapsr` tend to oversmooth the target functions owing to excessive penalization. Conversely, `mgcv` yields highly oscillatory estimates of the linear function, indicating a tendency towards overfitting for simpler functions. Both `R2BayesX` and `Blapsr` face challenges with locally varying smoothness, as penalized splines are not designed for such adaptability without substantial modifications (Crainiceanu et al., 2007; Jullion and Lambert, 2007; Scheipl and Kneib, 2009). We observe that `mgcv` with local adaptation performs well for estimating locally varying smoothness of  $f_2$ . However, performance summaries for  $f_1$  and  $f_3$  indicate that using `mgcv` for adaptive estimation may lead to higher RMSEs and incorrect



(a) Pointwise posterior mean estimates of  $f_1$  in 50 replications



(b) Pointwise posterior mean estimates of  $f_2$  in 50 replications



(c) Pointwise posterior mean estimates of  $f_3$  in 50 replications

Figure 6: Pointwise posterior means (gray) of  $f_1$ ,  $f_2$ , and  $f_3$  in the nonparametric logistic regression model with  $n = 1000$ , obtained from randomly chosen 50 replicated datasets, along with the true function (red).

coverage probabilities. Accordingly, a major drawback of `mgcv` arises from the need to accurately specify in advance whether to use adaptive estimation to achieve optimal performance, which is challenging because of the unknown characteristics of the target function.

Among the BMS-based approaches, the even-knot splines exhibit limitations in adapting to

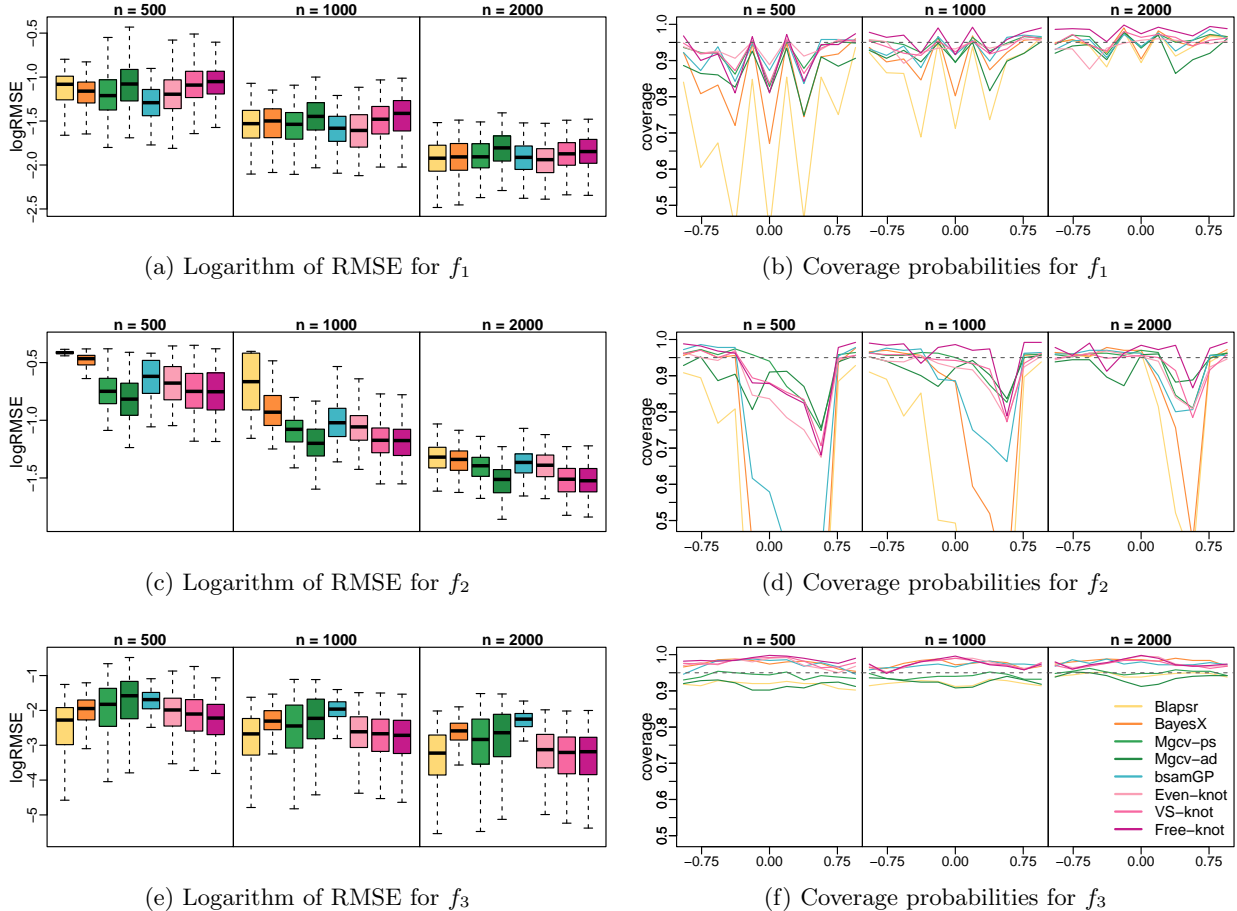


Figure 7: Logarithm of RMSE and coverage probabilities for  $f_1$ ,  $f_2$ , and  $f_3$  in the nonparametric logistic regression models with  $n = 500, 1000, 2000$ , obtained from 500 replicated datasets.

locally varying smoothness of  $f_2$  because of their construction with equidistant knots. In contrast, both the VS-knot and free-knot splines accurately identify the local features of  $f_2$ . The results indicate that the RMSEs of the two methods for adaptive estimation are comparable, with the free-knot splines tending to slightly overestimate coverage probabilities. Similar to the comparison between `mgcv-ps` and `mgcv-ad`, the even-knot splines outperform the VS-knot and free-knot splines in estimating  $f_1$ . However, the VS-knot splines perform better in estimating  $f_3$ , highlighting that the BMS-based methods are less sensitive to the specification of whether to use adaptive estimation in advance. Given that the VS-knot splines generally outperform other methods and demonstrate effective local adaptation, we recommend using the VS-knot splines as the default option. Nonetheless, it is worth mentioning that the even-knot splines approach is faster than the other BMS-based methods and also eliminates the need for MCMC when  $p$  is reasonably small.

We also assess the computational efficiency of the Bayesian methods based utilizing MCMC. Since `mgcv` follows a frequentist approach, it is excluded from the comparison. Additionally, `Blapsr` is omitted as it does not rely on MCMC. We calculate the effective sample sizes of the

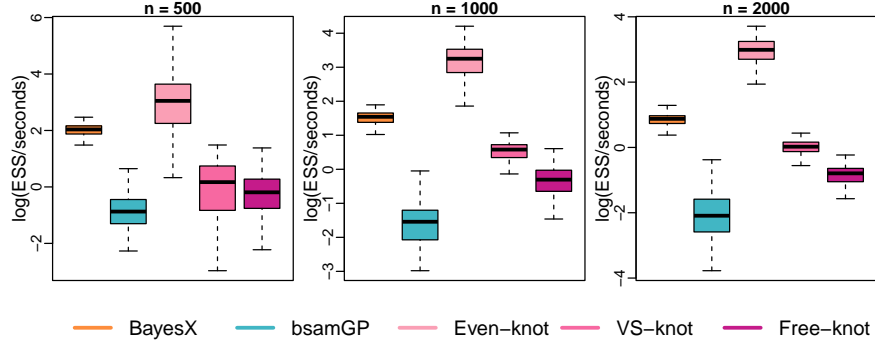


Figure 8: Logarithm of the effective sample sizes of the joint posterior per second of runtime, in the nonparametric logistic regression models with  $n = 500, 1000, 2000$ , obtained from 500 replicated datasets.

joint posterior per second of runtime after suitable burn-in periods. Figure 8 displays the efficiency measures across 500 replications. Contrary to the common belief that BMS-based methods may not be efficient, they are indeed comparable to other Bayesian methods. In particular, the even-knot splines emerge as the most efficient. This is attributed to the fact that, although BMS-based methods are slow, they exhibit fast mixing. While the VS-knot splines are slower than the even-knot splines, the trade-off appears reasonable, considering the ability for local adaptation.

## 6 Application to Pima diabetes data

In this section, we analyze the Pima datasets using the VS-knot splines approach with the intrinsic prior. The Pima diabetes dataset consists of signs of diabetes and seven potential risk factors of  $n = 532$  Pima Indian women in Arizona (Smith et al., 1988). We examine the relationship between the signs of diabetes and the risk factors using a GAM. The response variable  $Y_i$  indicates the presence of diabetes (0: negative, 1: positive). For each individual  $i$ , the predictor variables (risk factors) are  $pregnant_i$  (number of times the subject was pregnant),  $glucose_i$  (plasma glucose concentration in two hours in an oral glucose tolerance test [ $mg/dl$ ]),  $pressure_i$  (diastolic blood pressure [ $mm/Hg$ ]),  $triceps_i$  (triceps skin fold thickness [ $mm/Hg$ ]),  $mass_i$  (body mass index, BMI),  $pedigree_i$  (diabetes pedigree function), and  $age_i$  (age).

To examine the relationship between  $Y_i$  and the risk factors, we consider the following GAM with a logit link,

$$\begin{aligned} \log \frac{E(Y_i)}{1 - E(Y_i)} = & \alpha + f_1(pregnant_i) + f_2(glucose_i) + f_3(pressure_i) \\ & + f_4(triceps_i) + f_5(mass_i) + f_6(pedigree_i) + f_7(age_i). \end{aligned} \quad (18)$$

The individuals with missing values are removed from the analysis. The results, summarized in Figure 9, are largely consistent with the intuition. Many variables have near-linear effects but a few variables clearly have nonlinear effects, for example, the body mass index and age. The predictor variables with near-linear effects may instead be modeled using linear functions to reduce model complexity.

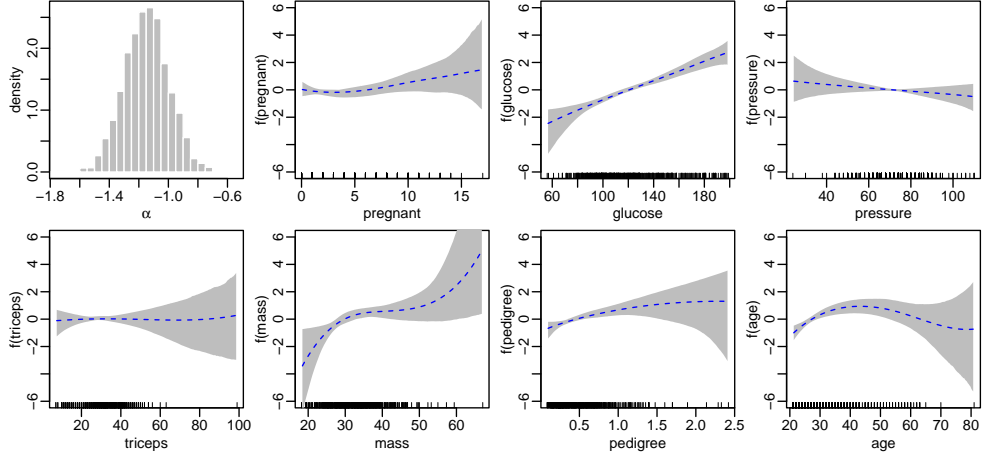


Figure 9: The posterior distribution of  $\alpha$  and the pointwise posterior means (blue dashed curve) and pointwise 95% credible bands (gray shade) of the functions  $f_j$ ,  $j = 1, \dots, 7$ , for the model in (18).

## 7 Discussion

This study considers the BMS-based estimation methods for GAMs using the Laplace approximation with mixtures of g-priors. In establishing a default prior, we elucidate the behavior of the Bayes factor and present various numerical results. As a byproduct, the study consolidates existing ideas on priors for knots and mixtures of g-priors.

The major bottleneck of our BMS-based approaches is the dependency on the maximum likelihood estimator, which leads to costly computation. Given that the VS-knot splines approach is shown to be sufficiently effective in this study, a potential remedy is employing shrinkage priors for exponential family models with a reasonable MCMC sampling algorithm (e.g., Schmidt and Makalic, 2020). Another possibility is exploring a computationally less expensive approximation to the likelihood (e.g., Rossell et al., 2021). As another extension, it may be advantageous to explore a higher-order approximation for improved approximation behavior (Shun and McCullagh, 1995).

## Acknowledgment

The research was supported by the Yonsei University Research Fund of 2021-22-0032 and the National Research Foundation of Korea (NRF) grant funded by the Korea government (MSIT) (2022R1C1C1006735, RS-2023-00217705).

## Supplementary material

### S1 Truncated compound confluent hypergeometric distributions

The truncated compound confluent hypergeometric (tCCH) distribution is formally defined by [Li and Clyde \(2018\)](#), as a slight modification of the generalized beta distribution defined by [Gordy \(1998b\)](#). Specifically, we write  $V \sim \text{tCCH}(a, b, z, s, \nu, \kappa)$  if  $V$  has a density of the form

$$f(v) = \frac{\nu^a u^{a-1} (1 - \nu u)^{b-1} [\kappa + (1 - \kappa)\nu u]^{-z} e^{s/\nu} e^{-su}}{\Phi_1(b, z, a + b, s/\nu, 1 - \kappa) B(a, b)} \mathbb{1}\{0 < u < 1/\nu\}. \quad (\text{S19})$$

where  $a > 0$ ,  $b > 0$ ,  $z \in \mathbb{R}$ ,  $s \in \mathbb{R}$ ,  $\nu \geq 1$  and  $\kappa > 0$ . A direct calculation gives the  $k$ th moment as

$$E(V^k) = \nu^{-k} \frac{B(a + k, b) \Phi_1(b, z, a + b + k, s/\nu, 1 - \kappa)}{B(a, b) \Phi_1(b, z, a + b, s/\nu, 1 - \kappa)}. \quad (\text{S20})$$

The tCCH distribution reduces to many distributions depending on the parameter values, such as a Gaussian hypergeometric distribution ([Armero and Bayarri, 1994](#)), confluent hypergeometric distribution ([Gordy, 1998a](#)), beta distribution, and gamma distribution. We refer the reader to the monograph by [Gupta and Nadarajah \(2004, p.132, p.279\)](#) for more details. Accordingly, the marginal likelihood in (11) is simplified depending on the parameters of the tCCH prior.

### S2 Proofs of the propositions

*Proof of Proposition 1.* Consider boundary knots  $\{t^L, t^U\}$  and interior knots  $\{t_1, \dots, t_M\}$  satisfying  $t^L < t_1 < \dots < t_M < t^U$ . To concatenate the expressions, we write  $t_0 = t^L$  and  $t_{M+1} = t^U$ . The common expression of the natural cubic splines derived from the truncated cubic spline basis functions is given by

$$N_1^*(u) = u, \\ N_{k+2}^*(u) = \frac{(u - t_k)_+^3 - (u - t_{M+1})_+^3}{t_{M+1} - t_k} - \frac{(u - t_M)_+^3 - (u - t_{M+1})_+^3}{t_{M+1} - t_M}, \quad k = 0, \dots, M-1,$$

(see, for example, equations (5.4) and (5.5) of [Hastie et al. \(2009\)](#)). Letting  $N_0^*(u) = 1$ , it is well known that  $\mathcal{N}^* = \{N_k^*, k = 0, 1, \dots, M+1\}$  is a basis for the cubic spline space with the natural boundary conditions. Therefore, it suffices to show that there exists an injection  $Q : \mathcal{N} \mapsto \mathcal{N}^*$ . As  $N_0 = N_0^*$ ,  $N_1 = N_1^*$ ,  $-N_{M+1} = N_2^*$  and  $N_{k-1} - N_{M+1} = N_k^*$ ,  $k = 3, \dots, M+1$ , we obtain

$$Q = \begin{pmatrix} 1 & 0 & 0 & 0 & \dots & 0 & 0 \\ 0 & 1 & 0 & 0 & \dots & 0 & 0 \\ 0 & 0 & 0 & 0 & \dots & 0 & -1 \\ 0 & 0 & 1 & 0 & \dots & 0 & -1 \\ 0 & 0 & 0 & 1 & \dots & 0 & -1 \\ \vdots & \vdots & \vdots & \vdots & \ddots & \vdots & \vdots \\ 0 & 0 & 0 & 0 & \dots & 1 & -1 \end{pmatrix},$$

which is clearly nonsingular. □

*Proof of Proposition 2.* Each of the basis terms  $N(\cdot; t^L, t^U, t_k)$ ,  $k = 1, \dots, M$ , in  $\mathcal{N}$  consists only of  $t^L$ ,  $t^U$ , and  $t_k$ . Hence, a new knot-point  $t_*$  introduces a new basis that is defined as  $N(\cdot; t^L, t^U, t_*)$  without altering other basis terms. Similarly, the elimination of an existing knot-point  $t_k$  removes the corresponding  $N(\cdot; t^L, t^U, t_k)$  without altering other terms.  $\square$

*Proof of Proposition 3.* Suppose the tCCH prior in (S19) is chosen. If  $\hat{\eta}_{\xi(1)} = \hat{\eta}_{\xi(2)}$ , we obtain that

$$\begin{aligned} BF[\xi(1); \xi(2)] &= \nu^{-k/2} \frac{B((a + J_{\xi(2)} + k)/2, b/2)}{B((a + J_{\xi(2)})/2, b/2)} \\ &\times \frac{\Phi_1(b/2, r, (a + b + J_{\xi(2)} + k)/2, (s + Q_{\xi(2)})/(2\nu), 1 - \kappa)}{\Phi_1(b/2, r, (a + b + J_{\xi(2)})/2, (s + Q_{\xi(2)})/(2\nu), 1 - \kappa)}, \end{aligned}$$

using the expression in (11). Given that the posterior of  $(g+1)^{-1}$  is the tCCH distribution in the first line of (12), the assertion is easily verified using (S20) if the tCCH prior is used for  $(g+1)^{-1}$ . A similar proof can be extended to the case of the unit information prior.  $\square$

### S3 Laplace approximation to the marginal likelihood

Following the proof of Proposition 1 of [Li and Clyde \(2018\)](#), the Laplace approximation to the likelihood yields

$$p(Y | \alpha, \beta_\xi, \xi) \approx p(Y | \hat{\eta}_\xi) \exp \left\{ -\frac{(\alpha - \hat{\alpha}_\xi + m)^2}{2\text{tr}(J_n(\hat{\eta}_\xi))} - \frac{1}{2}(\beta_\xi - \hat{\beta}_\xi)^T \tilde{B}_\xi^T J_n(\hat{\eta}_\xi) \tilde{B}_\xi (\beta_\xi - \hat{\beta}_\xi) \right\},$$

where  $m = \text{tr}(J_n(\hat{\eta}_\xi))^{-1} 1_n^T J_n(\hat{\eta}_\xi) B_\xi (\beta_\xi - \hat{\beta}_\xi)$ . Combined with the prior  $\pi(\alpha)\pi(\beta_\xi | g, \xi)$  in (7) and (8), this verifies the second and third lines of (12). Then, it is straightforward to see that

$$\begin{aligned} p(Y | g, \xi) &\approx \int \int \pi(\alpha)\pi(\beta_\xi | g, \xi) p(Y | \alpha, \beta_\xi, \xi) d\alpha d\beta_\xi \\ &= p(Y | \hat{\eta}_\xi) \text{tr}(J_n(\hat{\eta}_\xi))^{-1/2} (g+1)^{-J_\xi/2} \exp \left( -\frac{Q_\xi}{2(g+1)} \right), \end{aligned}$$

which verifies (9). Combined with the tCCH prior in (10), this verifies the first line of (12) using the density in (S19). Now, we can marginalize out  $g$ , that is,

$$\begin{aligned} p(Y | \xi) &\approx \frac{p(Y | \hat{\eta}_\xi) \text{tr}(J_n(\hat{\eta}_\xi))^{-1/2} \nu^{a/2} e^{s/(2\nu)} / B(a/2, b/2)}{\Phi_1(b/2, r, (a+b)/2, s/(2\nu), 1 - \kappa)} \int_0^{1/\nu} \frac{u^{(a+J_\xi)/2-1} (1 - \nu u)^{b/2-1}}{[\kappa + (1 - \kappa)\nu u]^r e^{(s+Q_\xi)u/2}} du \\ &= p(Y | \hat{\eta}_\xi) \text{tr}(J_n(\hat{\eta}_\xi))^{-1/2} \nu^{-J_\xi/2} \exp \left( -\frac{Q_\xi}{2\nu} \right) \frac{B((a+J_\xi)/2, b/2)}{B(a/2, b/2)} \\ &\times \Phi_1 \left( \frac{b}{2}, r, \frac{a+b+J_\xi}{2}, \frac{s+Q_\xi}{2\nu}, 1 - \kappa \right) / \Phi_1 \left( \frac{b}{2}, r, \frac{a+b}{2}, \frac{s}{2\nu}, 1 - \kappa \right), \end{aligned}$$

where the equality holds by the change of variables  $v = \nu u$ . This verifies (11).

## S4 Sampling from tCCH distributions

### S4.1 Exact sampling when $b = 1$ and $\kappa = 1$

Given (S19), the density of  $\text{tCCH}(a, 1, z, s, \nu, 1)$  has the form  $f(u) \propto u^{a-1} e^{-su} \mathbb{1}\{0 < u < 1/\nu\}$ , which is the gamma density truncated to  $0 < u < 1/\nu$ . Therefore, exact sampling from tCCH distributions is straightforward using the inverse transform method in this specific case. Combining the first line of (12) and Table 1, it is trivial that the posterior distribution  $\Pi((g+1)^{-1} | Y, \xi)$  is reduced to a truncated gamma distribution if the uniform, hyper-g, ZS-adapted, or robust prior is used.

### S4.2 Slice sampling when $z > 0$

The posterior distributions resulting from the hyper-g/n, beta-prime and intrinsic prior do not reduce to truncated gamma distributions. In such cases, we can employ a version of slice sampling.

To generate samples from  $V \sim \text{tCCH}(a, b, z, s, \nu, \kappa)$  with  $z > 0$ , we consider the change of variable  $W = \nu V$  with reparameterization  $\xi = \kappa^{-1} - 1$  and  $\zeta = s/\nu$ . It is easy to see that the density of  $W$  is given by

$$\begin{aligned} f(w) &\propto w^{a-1} (1-w)^{b-1} (1+\xi w)^{-z} e^{-\zeta w} \mathbb{1}\{0 < w < 1\} \\ &= w^{a-1} (1-w)^{b-1} e^{-\zeta w} \mathbb{1}\{0 < w < 1\} \Gamma(z)^{-1} \int_0^\infty t^{z-1} e^{-(1+\xi w)t} dt, \end{aligned}$$

where  $\Gamma$  is the gamma function. Therefore,  $f$  can be obtained as the marginal density from the joint density

$$\begin{aligned} h(w, t, u_1, u_2) &\propto w^{a-1} (1-w)^{b-1} t^{z-1} e^{-t} \\ &\quad \times \mathbb{1}\{0 < u_1 < e^{-\zeta w}\} \mathbb{1}\{0 < u_2 < e^{-\xi w t}\} \mathbb{1}\{0 < w < 1\}. \end{aligned}$$

Given that  $\xi > 0$  and  $\zeta > 0$ , a slice sampler is constructed as

$$\begin{aligned} U_1 | U_2, T, W &\sim \text{Unif}(0, e^{-\zeta W}), \\ U_2 | U_1, T, W &\sim \text{Unif}(0, e^{-\xi T W}), \\ T | U_1, U_2, W &\sim \text{Gamma}(z, 1) \times \mathbb{1}\{-\infty < T < -(\log U_2)/(\xi W)\}, \\ W | U_1, U_2, T &\sim \text{Beta}(a, b) \times \mathbb{1}\{-\min\{\log U_1, (\log U_2)/T\} < W < 1\}. \end{aligned}$$

## S5 Gaussian additive regression with unknown precision

Thus far, we have focused on GAMs with a known dispersion parameter  $\phi$  for the exponential family models. Now, we consider a more classical setup with a Gaussian assumption on the distribution of  $Y_i$ , while treating  $\phi$  as an unknown parameter. For Gaussian additive regression, a response variable  $Y_i$  is expressed as

$$Y_i = \alpha + \sum_{j=1}^p f_j(x_{ij}) + \epsilon_i, \quad \epsilon_i \sim N(0, \phi^{-1}), \quad i = 1, \dots, n, \quad (\text{S21})$$

where the precision parameter  $\phi$  is typically unknown. Although model (S21) also belongs to the GAM framework, there are distinctions due to the presence of the unknown precision parameter  $\phi$ . Let  $\eta = (\eta_1, \dots, \eta_n)^T$  be the vector of mean response, that is,  $\eta_i = E(Y_i)$ . We parameterize  $\eta$  as  $\eta = \alpha 1_n + B_\xi \beta_\xi$  using  $\alpha$ ,  $B_\xi$ , and  $\beta_\xi$  defined in Section 2. Following the convention, an improper prior is put on  $(\alpha, \phi)$ , that is,

$$\pi(\alpha, \phi) \propto 1/\phi.$$

Given that the information matrix of a Gaussian distribution is an identity matrix, one can easily check that the prior in (8) is reduced to the usual g-prior distribution (Zellner, 1986),

$$\beta_\xi \mid \phi, g, \xi \sim N(0, g\phi^{-1}(B_\xi^T B_\xi)^{-1}).$$

Observe that for the Gaussian case, we obtain  $\tilde{B}_\xi = B_\xi$  because the columns of  $B_\xi$  are centered.

Combining the marginal likelihood with one of the priors for  $\xi$  discussed in Section 4, we obtain the marginal posterior of  $\xi$ ,  $\Pi(\xi \mid Y)$ . The calculation of the marginal likelihood is complicated because  $\phi$  needs to be integrated along with  $g$ . First, it is well known that

$$p(Y \mid g, \xi) = p(Y \mid \emptyset) \frac{(1+g)^{(n-J_\xi-1)/2}}{[1+g(1-R_\xi^2)]^{(n-1)/2}}, \quad (\text{S22})$$

where  $p(Y \mid \emptyset) = n^{-1/2}(2\pi)^{-(n-1)/2}\Gamma((n-1)/2)(\|Y - \bar{Y}1_n\|^2/2)^{-(n-1)/2}$  is the marginal likelihood in the intercept-only model,  $R_\xi^2 = \|B_\xi(B_\xi^T B_\xi)^{-1}B_\xi^T Y\|^2/\|Y - \bar{Y}1_n\|^2$  is the coefficient of determination with  $\xi$ , and  $\bar{Y} = n^{-1} \sum_{i=1}^n Y_i$  is the average of the observations. For the unit information prior  $\Pi(g) = \delta_n(g)$ , the marginal likelihood  $p(Y \mid \xi)$  is readily available from the expression in (S22). Assigning the tCCH prior in (10) to  $(g+1)^{-1}$ , Li and Clyde (2018) shows that if  $r = 0$  (or  $\kappa = 1$  equivalently),

$$\begin{aligned} p(Y \mid \xi) &= \frac{p(Y \mid \emptyset)}{\nu^{J_\xi/2}[1 - (1 - \nu^{-1})R_\xi^2]^{(n-1)/2}} \frac{B((a+J_\xi)/2, b/2)}{B(a/2, b/2)} \\ &\quad \times \Phi_1\left(\frac{b}{2}, \frac{n-1}{2}, \frac{a+b+J_\xi}{2}, \frac{s}{2\nu}, \frac{R_\xi^2}{\nu - (\nu-1)R_\xi^2}\right) / {}_1F_1\left(\frac{b}{2}, \frac{a+b}{2}, \frac{s}{2\nu}\right), \end{aligned}$$

and if  $s = 0$ ,

$$\begin{aligned} p(Y \mid \xi) &= \frac{p(Y \mid \emptyset)\kappa^{(a+J_\xi-2r)/2}}{\nu^{J_\xi/2}(1-R_\xi^2)^{(n-1)/2}} \frac{B((a+J_\xi)/2, b/2)}{B(a/2, b/2)} \\ &\quad \times F_1\left(\frac{a+J_\xi}{2}; \frac{a+b+J_\xi+1-n-2r}{2}, \frac{n-1}{2}; \right. \\ &\quad \left. \frac{a+b+J_\xi}{2}; 1-\kappa, 1-\kappa - \frac{R_\xi^2\kappa}{(1-R_\xi^2)v}\right) / {}_2F_1\left(r, \frac{b}{2}; \frac{a+b}{2}; 1-\kappa\right), \end{aligned}$$

where  ${}_1F_1(\alpha, \gamma, x) = \Phi_1(\alpha, 0, \gamma, x, 0)$ ,  $\gamma > \alpha > 0$ , is the confluent hypergeometric function,  ${}_2F_1(\beta, \alpha; \gamma; y) = \Phi_1(\alpha, \beta, \gamma, 0, y)$ ,  $\gamma > \alpha > 0$ , is the Gaussian hypergeometric function, and  $F_1$  is the the Appell hypergeometric function defined as  $F_1(\alpha; \beta, \beta'; \gamma; x, y) = B(\gamma-\alpha, \alpha)^{-1} \int_0^1 u^{\alpha-1} (1-u)^{\gamma-\alpha-1} (1-xu)^{-\beta} (1-yu)^{-\beta'} du$  for  $\gamma > \alpha > 0$ . The prior distributions listed in Table 1 fall

into one of the above two cases. The expressions may be further simplified depending on the hyperparameters of the tCCH prior, but numerical evaluation of the transcendental functions is often necessary. The only exception is the beta-prime prior, which provides a closed-form expression for the marginal likelihood without a hypergeometric-type transcendental function; see [Maruyama and George \(2011\)](#).

In the Gaussian case, the conditional posterior  $\Pi((g + 1)^{-1} | Y, \xi)$  is no longer a conjugate update of the tCCH prior. Nonetheless, it can be simplified with certain hyperparameter specifications of the tCCH prior, and sampling from  $\Pi((g + 1)^{-1} | Y, \xi)$  can be easily executed by introducing auxiliary variables. In particular, the beta-prime prior provides an exact sampling scheme from a beta distribution; see [Jeong et al. \(2022\)](#). The remaining specification of the joint posterior can easily be derived by direct calculations as

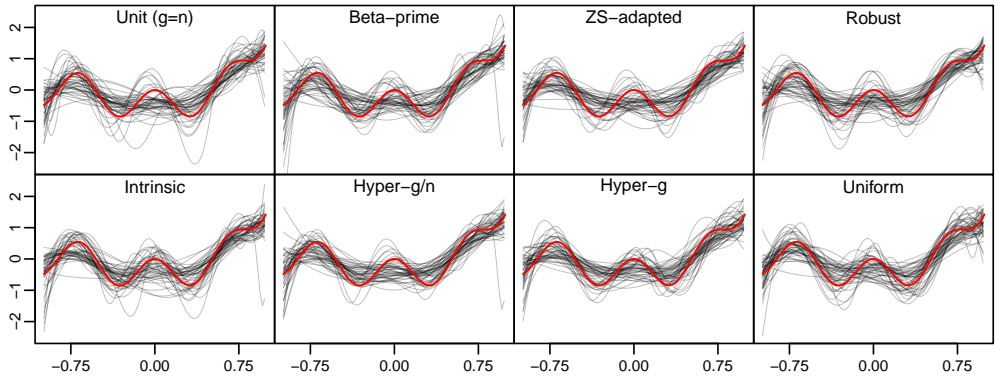
$$\begin{aligned}\phi | Y, g, \xi &\sim \text{Gamma}\left(\frac{n-1}{2}, \frac{\|Y - \bar{Y}1_n\|^2[1 + g(1 - R_\xi^2)]}{2(1+g)}\right), \\ \alpha | Y, \phi, g, \xi &\sim N(\bar{Y}, \phi^{-1}/n), \\ \beta_\xi | Y, \phi, g, \xi &\sim N\left(\frac{g}{g+1}\hat{\beta}_\xi, \frac{g\phi^{-1}}{g+1}(B_\xi^T B_\xi)^{-1}\right).\end{aligned}$$

The marginal posterior of  $\xi$ ,  $\Pi(\xi | Y)$ , is easily obtained from the above expressions of the marginal likelihood.

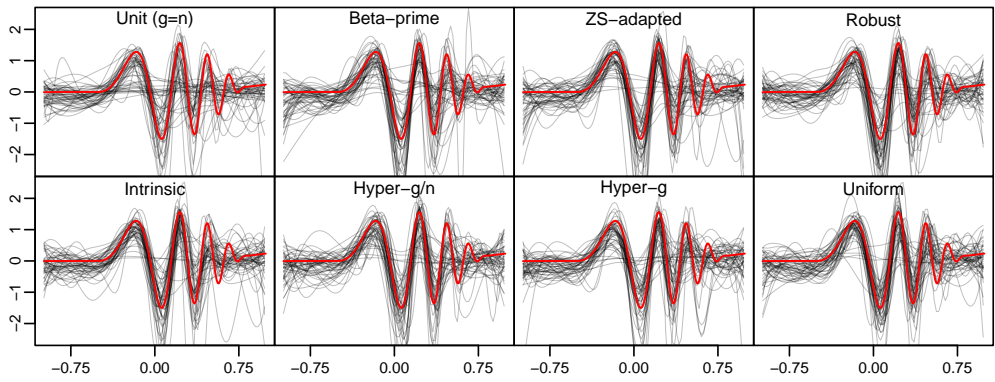
## S6 Simulation for Poisson and Gaussian regression

Section 5 exclusively presents simulations for a nonparametric logistic regression model. Given that the modeling framework encompasses a broad class of exponential family models, it is pertinent to investigate the properties of BMS-based methods for other GAMs. In this section, we present additional simulation results for the Poisson and Gaussian regression models. Similar to Section 5, the observations are generated with the linear predictor  $\eta_i = \alpha + \sum_{j=1}^3 f_j(x_{ij})$ , where  $f_j$  is the centered version of  $f_j^*$  in (17) and  $\alpha$  is the intercept induced by the centering. For Poisson regression,  $Y_i \sim \text{Poi}(e^{\eta_i})$ . For Gaussian regression,  $Y_i = \eta_i + \epsilon_i$  where  $\epsilon_i \sim N(0, 1)$ . We generate 500 replicated datasets of size  $n = 50, 100, 200$  for Poisson regression and  $n = 100, 200, 400$  for Gaussian regression. For each dataset, we employ the VS-knot splines approach to examine differences between the mixtures of g-priors. Additionally, we compare the BMS-based methods with the intrinsic prior to other Bayesian methods, substantiating the validity of BMS-based approaches.

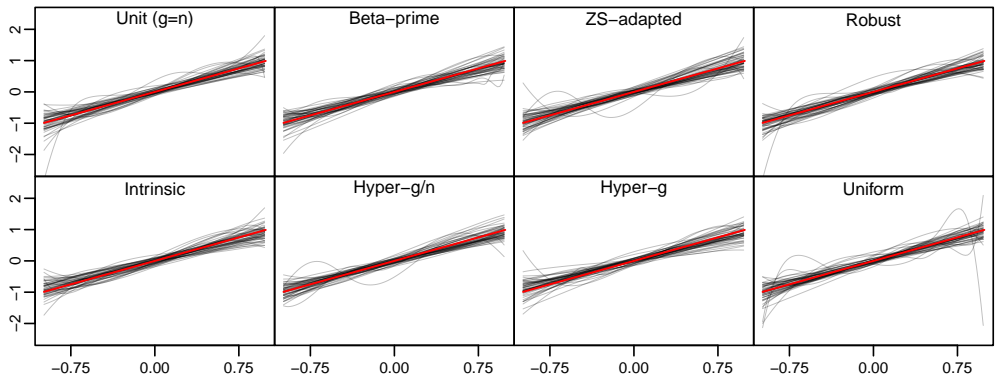
The simulation results are presented in Figures 10–17. Specifically, Figures 10–13 display the performance differences among the mixtures of g-priors in the VS-knot splines. Meanwhile, Figures 14–17 illustrate the comparison between the BMS-based methods and other Bayesian approaches. As `Blapsr` necessitates a known value of  $\phi$  in Gaussian regression, it is excluded from the comparison for Gaussian regression. The overall simulation performance aligns with the results for the logistic regression model in Section 5, leading to the similar conclusion. Similar to Section 5, the computational efficiency is also assessed through the effective samples sizes of the joint posterior per second of runtime. The efficiency performance measures are summarized in Figure 18. The conclusion remains essentially identical to that drawn in Section 5.



(a) Pointwise posterior mean estimates of  $f_1$  in 50 replications



(b) Pointwise posterior mean estimates of  $f_2$  in 50 replications



(c) Pointwise posterior mean estimates of  $f_3$  in 50 replications

Figure 10: Pointwise posterior means (gray) of  $f_1$ ,  $f_2$ , and  $f_3$  in the nonparametric Poisson regression model with  $n = 100$ , obtained from randomly chosen 50 replicated datasets, along with the true function (red).

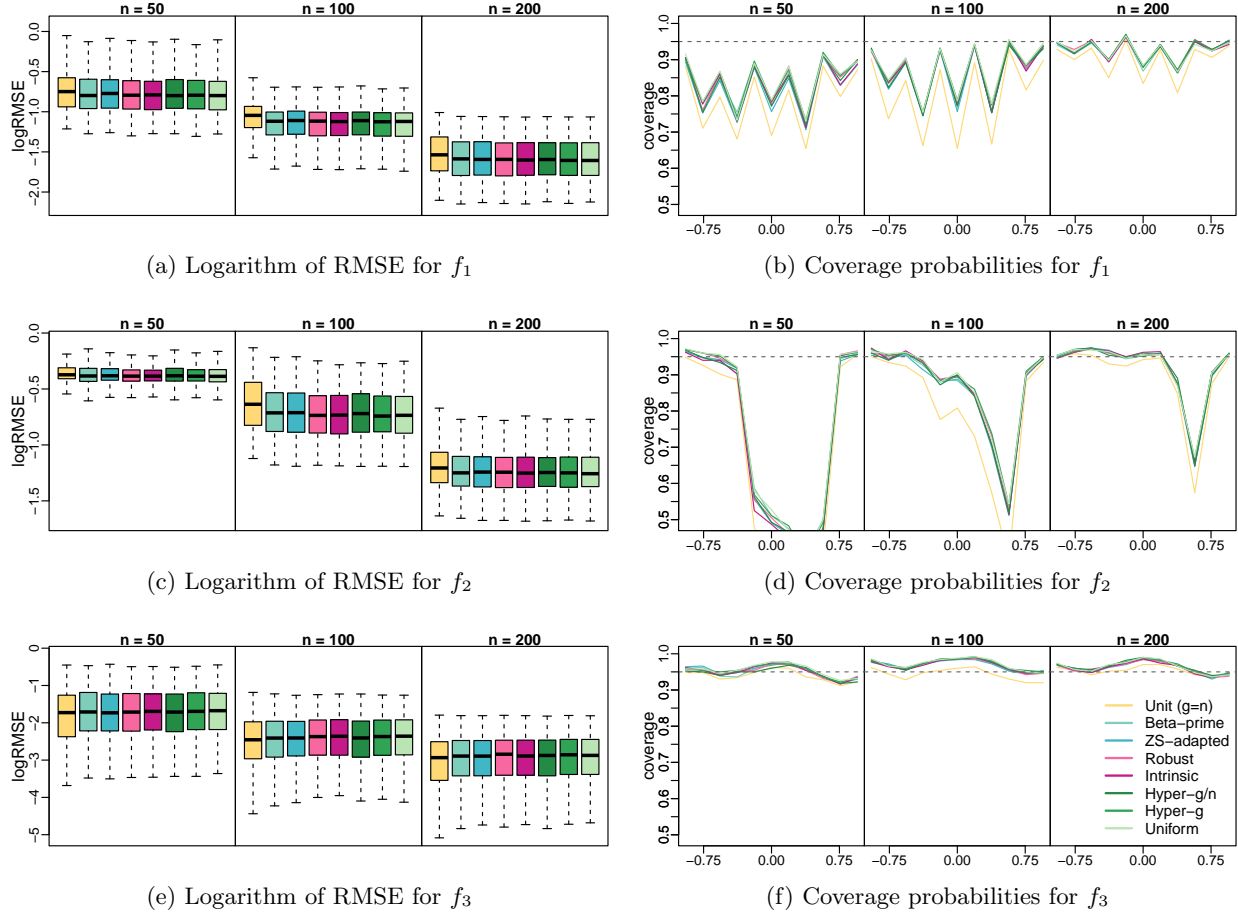
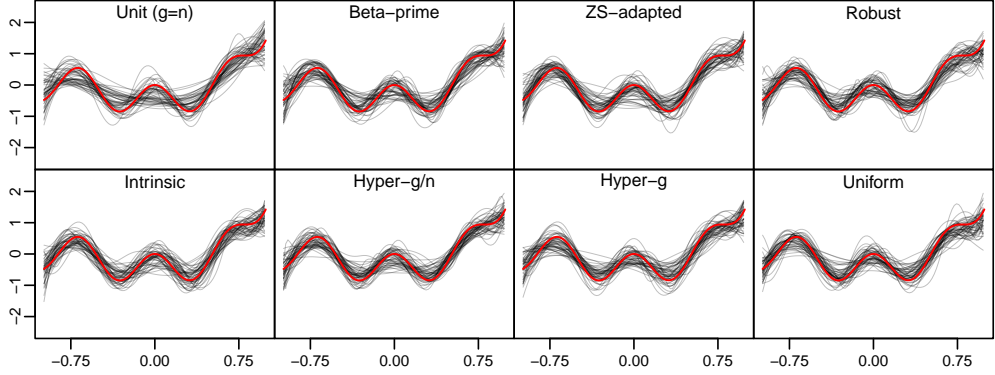
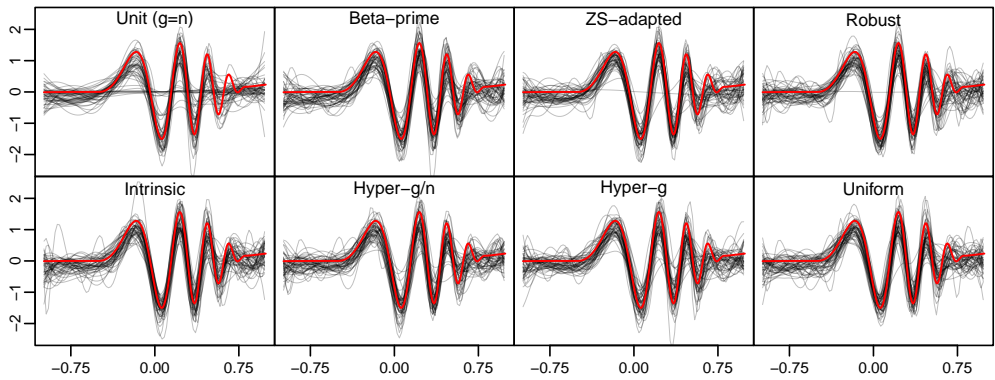


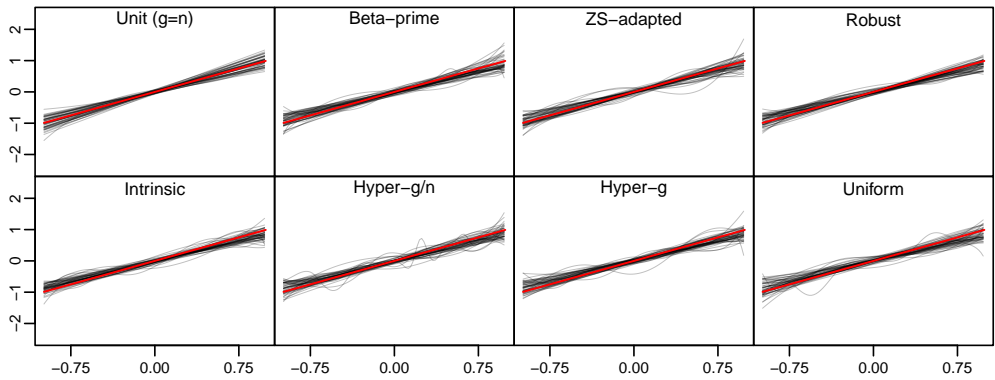
Figure 11: Logarithm of RMSE and coverage probabilities for  $f_1$ ,  $f_2$ , and  $f_3$  in the nonparametric Poisson regression models with  $n = 50, 100, 200$ , obtained from 500 replicated datasets.



(a) Pointwise posterior mean estimates of  $f_1$  in 50 replications



(b) Pointwise posterior mean estimates of  $f_2$  in 50 replications



(c) Pointwise posterior mean estimates of  $f_3$  in 50 replications

Figure 12: Pointwise posterior means (gray) of  $f_1$ ,  $f_2$ , and  $f_3$  in the nonparametric Gaussian regression model with  $n = 200$ , obtained from randomly chosen 50 replicated datasets, along with the true function (red).

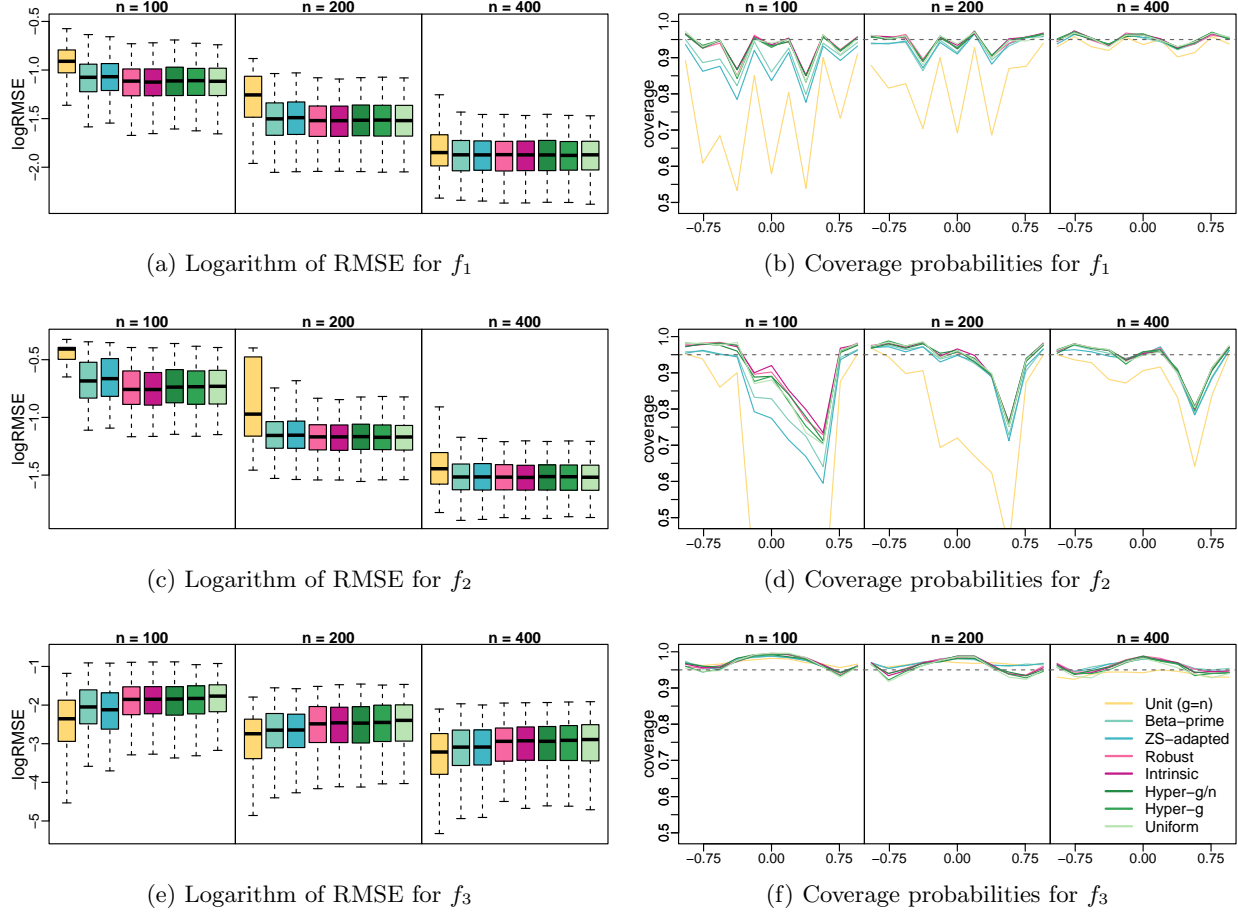
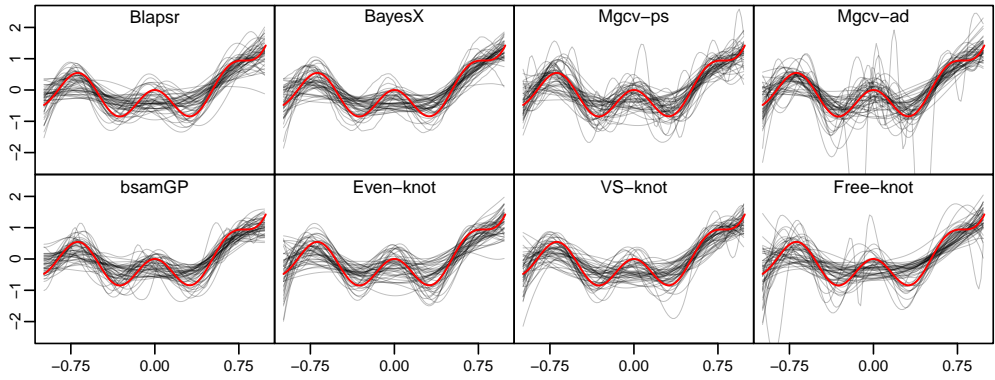
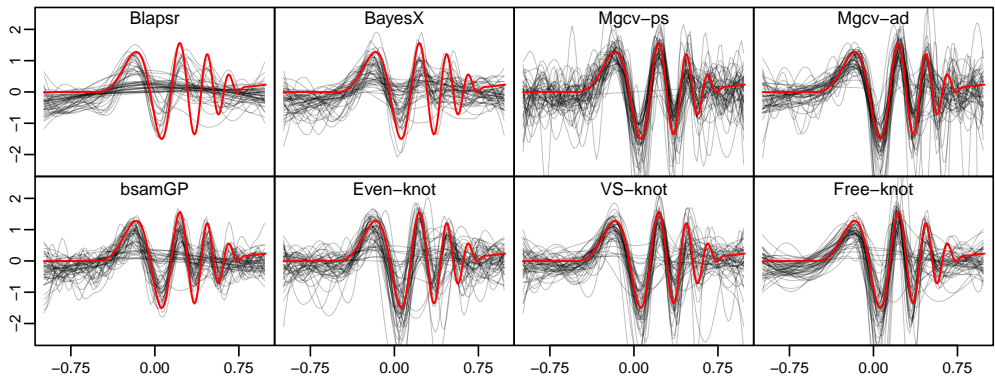


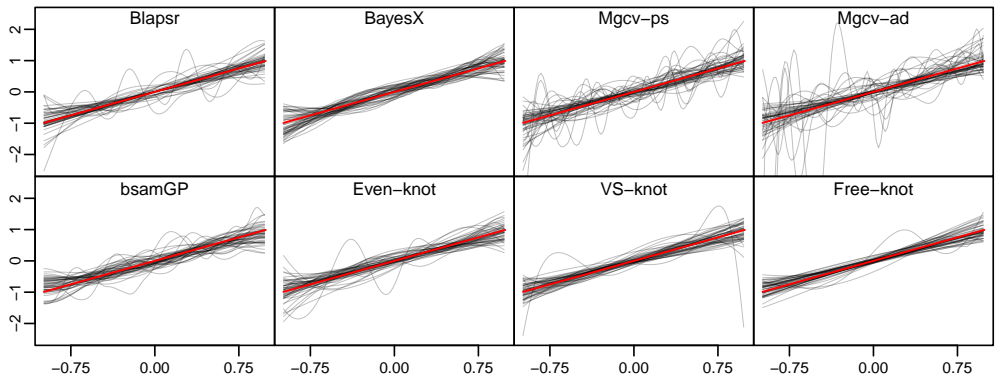
Figure 13: Logarithm of RMSE and coverage probabilities for  $f_1$ ,  $f_2$ , and  $f_3$  in the nonparametric Gaussian regression models with  $n = 100, 200, 400$ , obtained from 500 replicated datasets.



(a) Pointwise posterior mean estimates of  $f_1$  in 50 replications



(b) Pointwise posterior mean estimates of  $f_2$  in 50 replications



(c) Pointwise posterior mean estimates of  $f_3$  in 50 replications

Figure 14: Pointwise posterior means (gray) of  $f_1$ ,  $f_2$ , and  $f_3$  in the nonparametric Poisson regression model with  $n = 100$ , obtained from randomly chosen 50 replicated datasets, along with the true function (red).

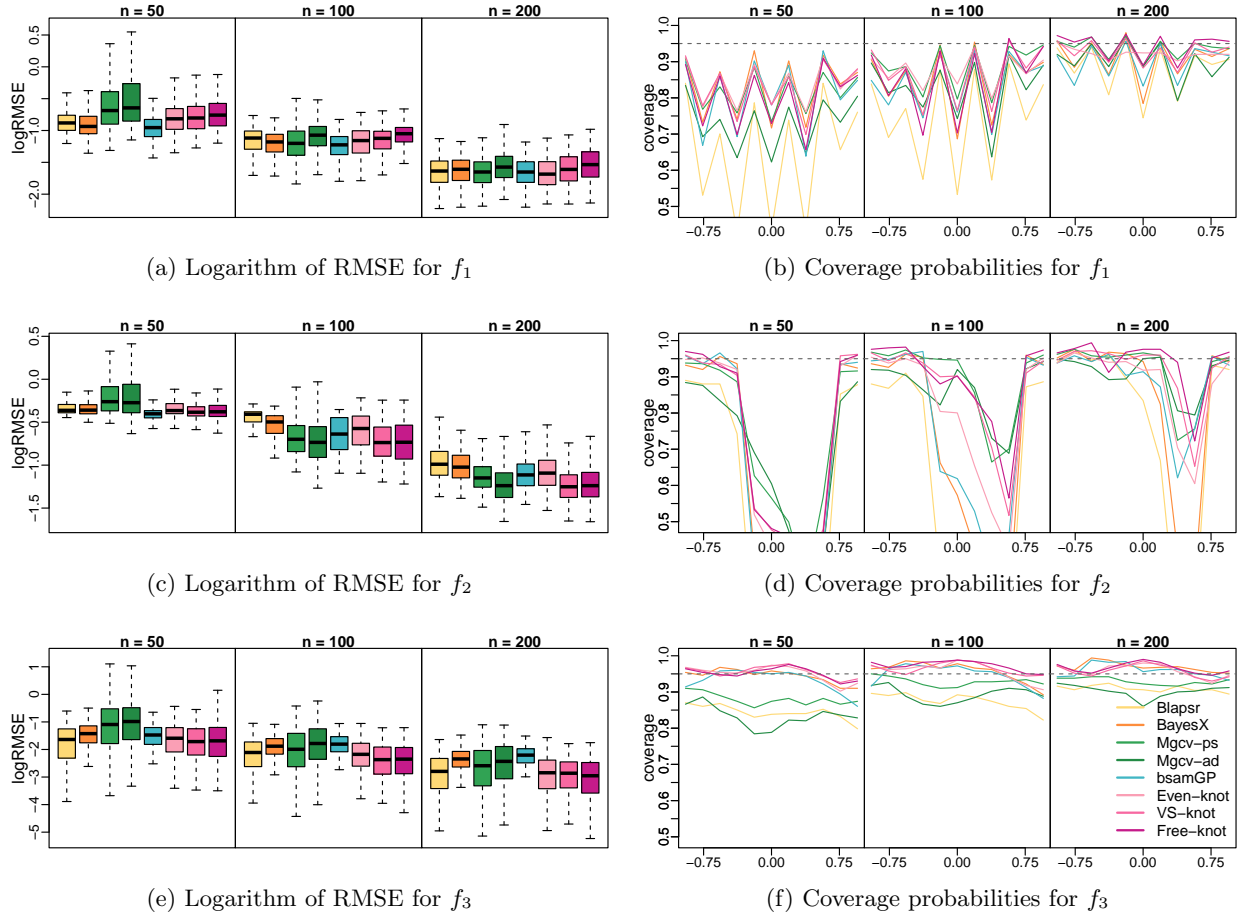
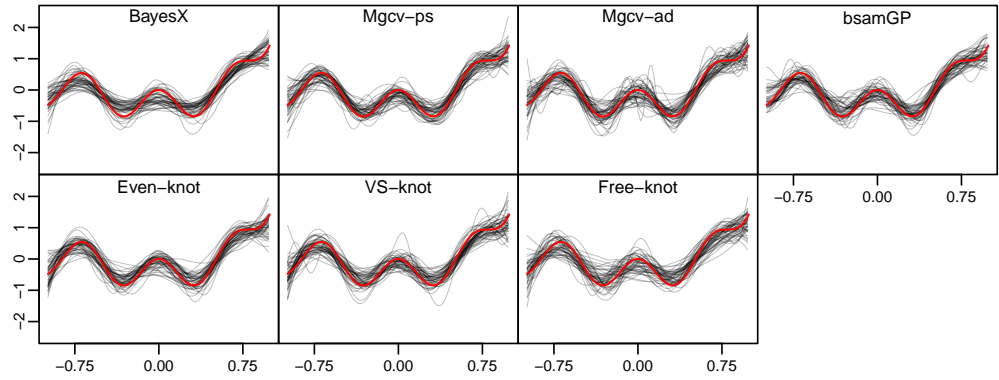
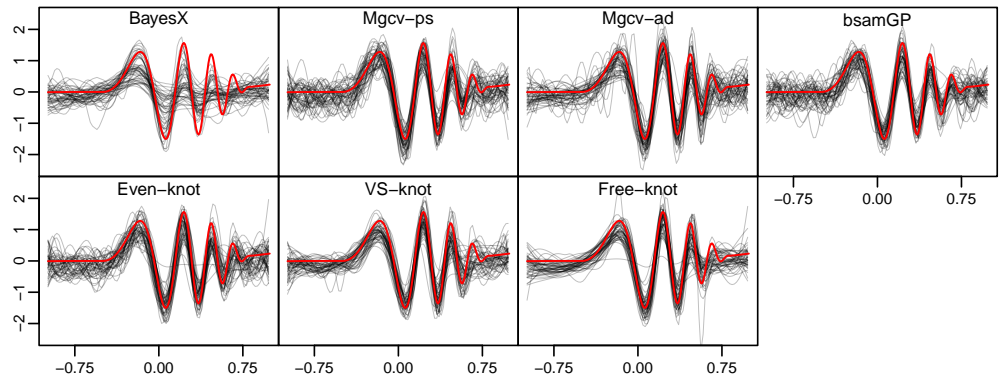


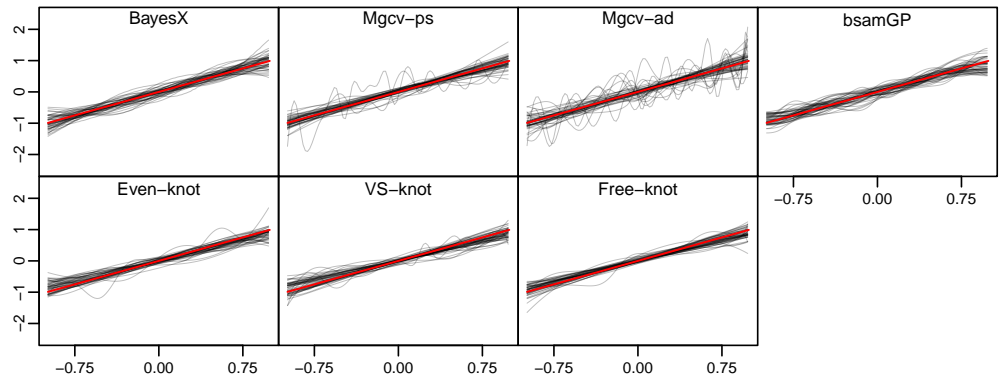
Figure 15: Logarithm of RMSE and coverage probabilities for  $f_1$ ,  $f_2$ , and  $f_3$  in the nonparametric Poisson regression models with  $n = 50, 100, 200$ , obtained from 500 replicated datasets.



(a) Pointwise posterior mean estimates of  $f_1$  in 50 replications



(b) Pointwise posterior mean estimates of  $f_2$  in 50 replications



(c) Pointwise posterior mean estimates of  $f_3$  in 50 replications

Figure 16: Pointwise posterior means (gray) of  $f_1$ ,  $f_2$ , and  $f_3$  in the nonparametric Gaussian regression model with  $n = 200$ , obtained from randomly chosen 50 replicated datasets, along with the true function (red).

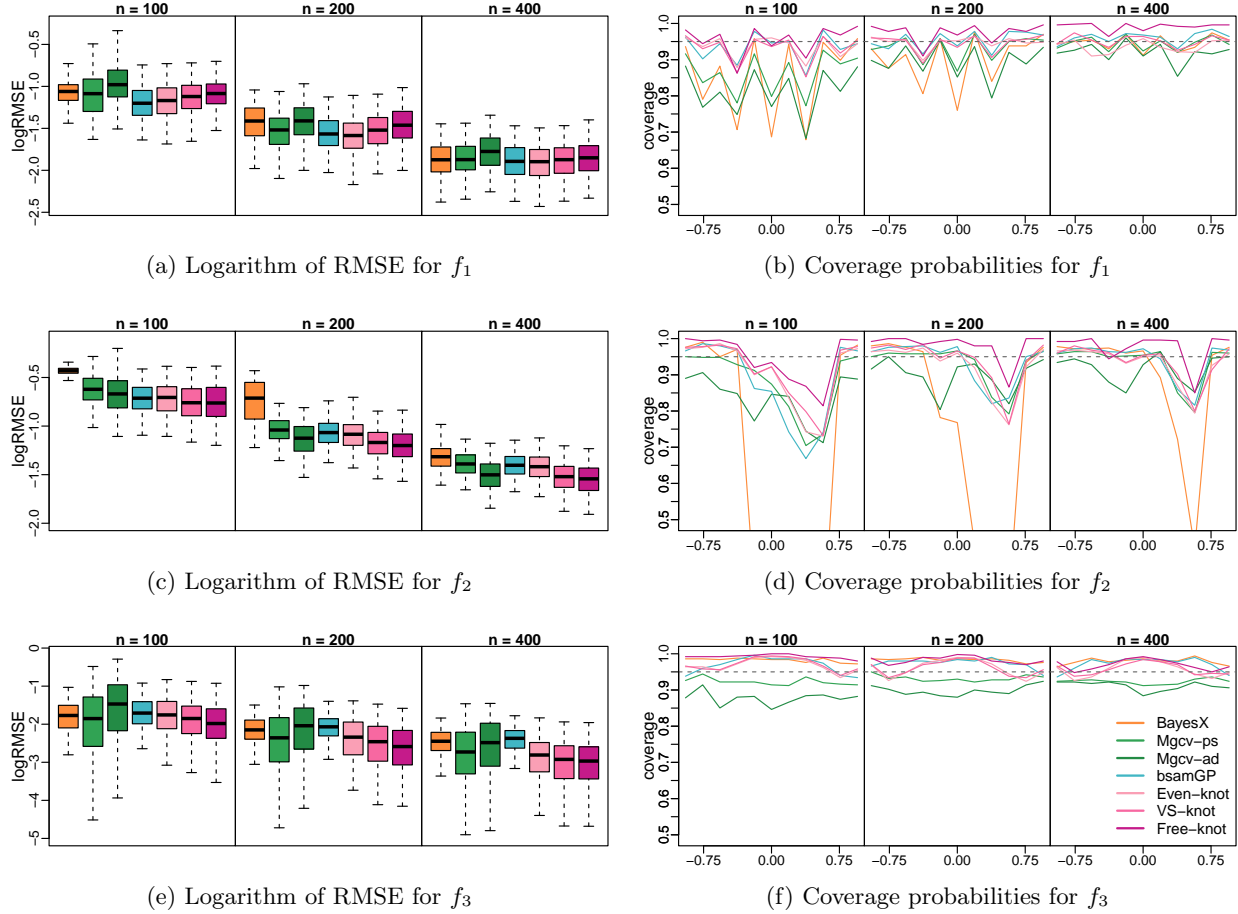
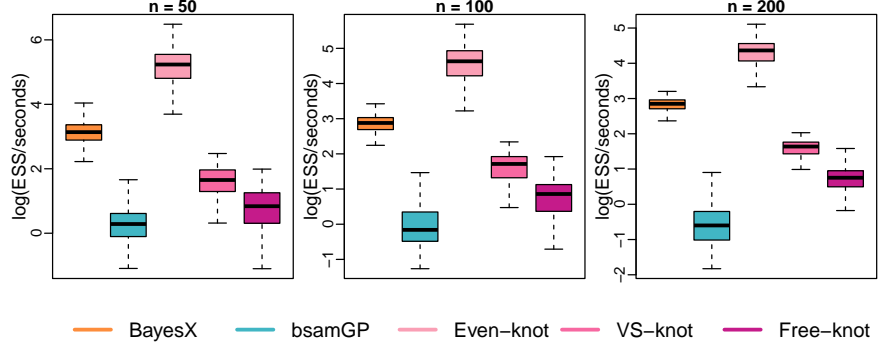
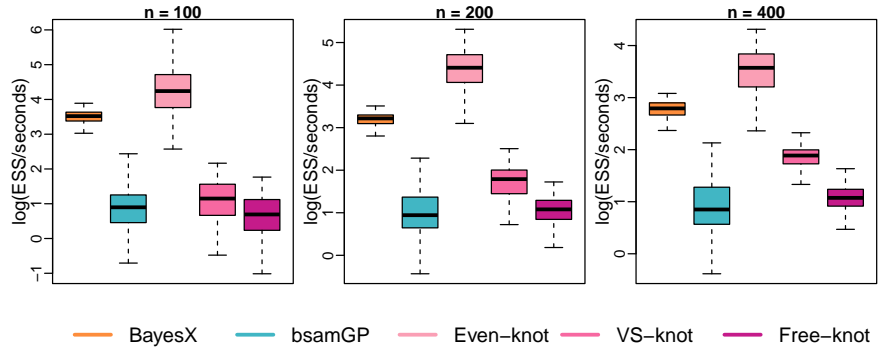


Figure 17: Logarithm of RMSE and coverage probabilities for  $f_1$ ,  $f_2$ , and  $f_3$  in the nonparametric Gaussian regression models with  $n = 100, 200, 400$ , obtained from 500 replicated datasets.



(a) Sampling efficiency in the Poisson regression models



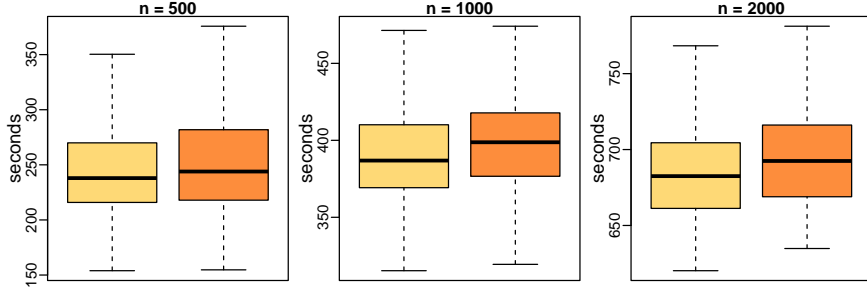
(b) Sampling efficiency in the Gaussian regression models

Figure 18: Logarithm of the effective sample sizes of the joint posterior per second of runtime, in the Poisson regression models with  $n = 50, 100, 200$  and the Gaussian regression models with  $n = 100, 200, 400$ , obtained from 500 replicated datasets.

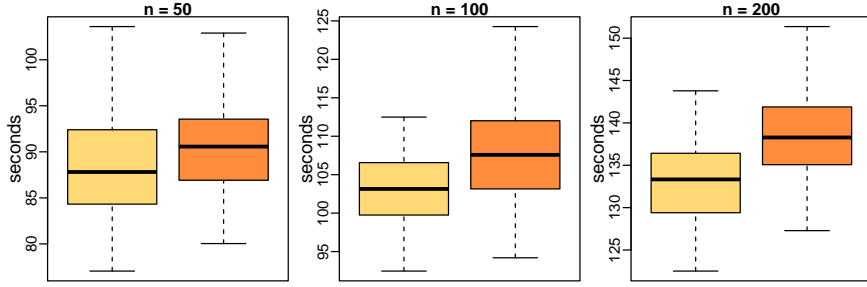
## S7 Simulation for basis construction

Proposition 2 suggests that our natural cubic spline basis in (4) is desirable in the VS-knot and free-knot splines. We now perform a numerical study to demonstrate the computational efficiency of the proposed basis construction. The simulation setups are identical to those in Section 5.1 and Section S6. Along with the basis construction in (4), we consider using the widely used truncated power natural cubic splines given in equations (5.4) and (5.5) in [Hastie et al. \(2009\)](#). In our simulation, both basis constructions are used for the VS-knot splines.

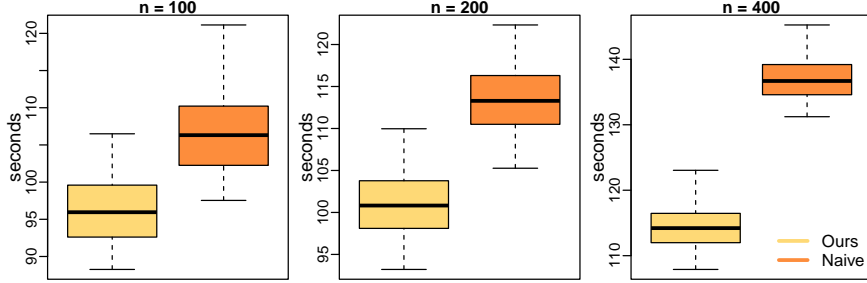
Figure 19 compares the computation time of the simulation using both basis constructions over 500 replications. (We only need to examine the computation runtime, as the two basis constructions yield exactly the same performance.) The runtime is measured under the system with an AMD Ryzen 5 3500X 6-Core processor. The figure shows that our basis construction facilitates the computation time. In particular, the relative time improvement is more pronounced in Gaussian regression than in the logistic and Poisson regression models. This is attributed to the fact that logistic and Poisson regression models involve more extensive computation because of the requirement for calculating the maximum likelihood estimates in every iteration of MCMC.



(a) Logistic regression



(b) Poisson regression



(c) Gaussian regression

Figure 19: Comparison of computation time between our basis construction (Ours) between the naive one given in [Hastie et al. \(2009\)](#) (Naive) using the VS-knot splines.

In contrast, Gaussian regression is computationally less demanding as the maximum likelihood estimate is unnecessary, resulting in a larger proportion of the computation time being dedicated to the basis construction compared to the other cases.

## S8 R package GAMBMS

Here, we show how to use the R package for the BMS-based approaches for GAMs. Using the `devtools` package available at CRAN, our R package can be installed and loaded by running the following code:

```
devtools::install_github("hun-learning94/gambms")
library(gambms)
```

One can reproduce the results given in Sections 5 and 6 by running the examples in the help page of the R function `gambms`.

## References

Armero, C. and Bayarri, M. (1994). Prior assessments for prediction in queues. *Journal of the Royal Statistical Society: Series D (The Statistician)*, 43(1):139–153.

Bayarri, M. J., Berger, J. O., Forte, A., and García-Donato, G. (2012). Criteria for Bayesian model choice with application to variable selection. *The Annals of Statistics*, 40(3):1550–1577.

Berger, J. O., Pericchi, L. R., and Varshavsky, J. A. (1998). Bayes factors and marginal distributions in invariant situations. *Sankhyā: The Indian Journal of Statistics, Series A*, pages 307–321.

Brezger, A. and Lang, S. (2006). Generalized structured additive regression based on Bayesian P-splines. *Computational Statistics & Data Analysis*, 50(4):967–991.

Chan, D., Kohn, R., Nott, D., and Kirby, C. (2006). Locally adaptive semiparametric estimation of the mean and variance functions in regression models. *Journal of Computational and Graphical Statistics*, 15(4):915–936.

Chen, M.-H. and Ibrahim, J. G. (2003). Conjugate priors for generalized linear models. *Statistica Sinica*, pages 461–476.

Cox, D. and Snell, E. (1989). *The Analysis of Binary Data*, volume 32. CRC Press.

Crainiceanu, C. M., Ruppert, D., Carroll, R. J., Joshi, A., and Goodner, B. (2007). Spatially adaptive Bayesian penalized splines with heteroscedastic errors. *Journal of Computational and Graphical Statistics*, 16(2):265–288.

Cripps, E., Carter, C., and Kohn, R. (2005). Variable selection and covariance selection in multivariate regression models. *Handbook of Statistics*, 25:519–552.

De Jonge, R. and Van Zanten, J. (2012). Adaptive estimation of multivariate functions using conditionally Gaussian tensor-product spline priors. *Electronic Journal of Statistics*, 6:1984–2001.

Dellaportas, P., Forster, J. J., and Ntzoufras, I. (2002). On Bayesian model and variable selection using MCMC. *Statistics and Computing*, 12(1):27–36.

Denison, D., Mallick, B., and Smith, A. (1998). Automatic Bayesian curve fitting. *Journal of the Royal Statistical Society: Series B (Statistical Methodology)*, 60(2):333–350.

DiMatteo, I., Genovese, C. R., and Kass, R. E. (2001). Bayesian curve-fitting with free-knot splines. *Biometrika*, 88(4):1055–1071.

Fahrmeir, L. and Lang, S. (2001). Bayesian inference for generalized additive mixed models based on Markov random field priors. *Journal of the Royal Statistical Society: Series C (Applied Statistics)*, 50(2):201–220.

Fouskakis, D., Ntzoufras, I., and Perrakis, K. (2018). Power-expected-posterior priors for generalized linear models. *Bayesian Analysis*, 13(3):721–748.

Francom, D. and Sansó, B. (2020). BASS: An R package for fitting and performing sensitivity analysis of Bayesian adaptive spline surfaces. *Journal of Statistical Software*, 94(8):1–36.

Francom, D., Sansó, B., Kupresanin, A., and Johannesson, G. (2018). Sensitivity analysis and emulation for functional data using Bayesian adaptive splines. *Statistica Sinica*, pages 791–816.

Gordy, M. B. (1998a). Computationally convenient distributional assumptions for common-value auctions. *Computational Economics*, 12(1):61–78.

Gordy, M. B. (1998b). A generalization of generalized beta distributions. Division of Research and Statistics, Division of Monetary Affairs, Federal Reserve Boards.

Green, P. J. (1995). Reversible jump Markov Chain Monte Carlo computation and Bayesian model determination. *Biometrika*, 82(4):711–732.

Gressani, O. and Lambert, P. (2021). Laplace approximations for fast Bayesian inference in generalized additive models based on P-splines. *Computational Statistics & Data Analysis*, 154:107088.

Gupta, A. K. and Nadarajah, S. (2004). *Handbook of Beta Distribution and Its Applications*. CRC press.

Gupta, M. and Ibrahim, J. G. (2009). An information matrix prior for Bayesian analysis in generalized linear models with high dimensional data. *Statistica Sinica*, 19(4):1641–1663.

Gustafson, P. (2000). Bayesian regression modeling with interactions and smooth effects. *Journal of the American Statistical Association*, 95(451):795–806.

Hansen, M. H. and Yu, B. (2003). Minimum description length model selection criteria for generalized linear models. *Lecture Notes-Monograph Series*, pages 145–163.

Hastie, T. and Tibshirani, R. (1986). Generalized additive models. *Statistical Sicence*, pages 297–318.

Hastie, T., Tibshirani, R., Friedman, J. H., and Friedman, J. H. (2009). *The Elements of Statistical Learning: Data Mining, Inference, and Prediction*. Springer, second edition.

Held, L., Sabanés Bové, D., and Gravestock, I. (2015). Approximate Bayesian model selection with the deviance statistic. *Statistical Science*, pages 242–257.

Jeong, S., Park, M., and Park, T. (2017). Analysis of binary longitudinal data with time-varying effects. *Computational Statistics & Data Analysis*, 112:145–153.

Jeong, S. and Park, T. (2016). Bayesian semiparametric inference on functional relationships in linear mixed models. *Bayesian Analysis*, 11(4):1137–1163.

Jeong, S., Park, T., and van Dyk, D. A. (2022). Bayesian model selection in additive partial linear models via locally adaptive splines. *Journal of Computational and Graphical Statistics*, 31(2):324–336.

Ji, C. and Schmidler, S. C. (2013). Adaptive Markov Chain Monte Carlo for Bayesian variable selection. *Journal of Computational and Graphical Statistics*, 22(3):708–728.

Jo, S., Choi, T., Park, B., and Lenk, P. (2019). bsampg: An R package for Bayesian spectral analysis models using Gaussian process priors. *Journal of Statistical Software*, 90(10):1–41.

Jullion, A. and Lambert, P. (2007). Robust specification of the roughness penalty prior distribution in spatially adaptive Bayesian P-splines models. *Computational Statistics & Data Analysis*, 51(5):2542–2558.

Kass, R. E. and Raftery, A. E. (1995). Bayes factors. *Journal of the American Statistical Association*, 90(430):773–795.

Kass, R. E. and Wasserman, L. (1995). A reference Bayesian test for nested hypotheses and its relationship to the Schwarz criterion. *Journal of the American Statistical Association*, 90(431):928–934.

Kohn, R., Smith, M., and Chan, D. (2001). Nonparametric regression using linear combinations of basis functions. *Statistics and Computing*, 11(4):313–322.

Lang, S. and Brezger, A. (2004). Bayesian P-splines. *Journal of Computational and Graphical Statistics*, 13(1):183–212.

Li, Y. and Clyde, M. A. (2018). Mixtures of g-priors in generalized linear models. *Journal of the American Statistical Association*, 113(524):1828–1845.

Liang, F., Paulo, R., Molina, G., Clyde, M. A., and Berger, J. O. (2008). Mixtures of g priors for Bayesian variable selection. *Journal of the American Statistical Association*, 103(481):410–423.

Magee, L. (1990).  $R^2$  measures based on Wald and likelihood ratio joint significance tests. *The American Statistician*, 44(3):250–253.

Maruyama, Y. and George, E. I. (2011). Fully Bayes factors with a generalized g-prior. *The Annals of Statistics*, 39(5):2740–2765.

Nagelkerke, N. J. (1991). A note on a general definition of the coefficient of determination. *Biometrika*, 78(3):691–692.

Nott, D. J. and Kohn, R. (2005). Adaptive sampling for Bayesian variable selection. *Biometrika*, 92(4):747–763.

Park, T. and Jeong, S. (2018). Analysis of Poisson varying-coefficient models with autoregression. *Statistics*, 52(1):34–49.

Rivoirard, V. and Rousseau, J. (2012). Posterior concentration rates for infinite dimensional exponential families. *Bayesian Analysis*, 7(2):311–334.

Rossell, D., Abril, O., and Bhattacharya, A. (2021). Approximate Laplace approximations for scalable model selection. *Journal of the Royal Statistical Society: Series B (Statistical Methodology)*, 83(4):853–879.

Sabanés Bové, D. and Held, L. (2011). Hyper- $g$  priors for generalized linear models. *Bayesian Analysis*, 6(3):387–410.

Sabanés Bové, D., Held, L., and Kauermann, G. (2015). Objective Bayesian model selection in generalized additive models with penalized splines. *Journal of Computational and Graphical Statistics*, 24(2):394–415.

Scheipl, F. and Kneib, T. (2009). Locally adaptive Bayesian P-splines with a Normal-Exponential-Gamma prior. *Computational Statistics & Data Analysis*, 53(10):3533–3552.

Schmidt, D. F. and Makalic, E. (2020). Bayesian generalized horseshoe estimation of generalized linear models. In *Joint European Conference on Machine Learning and Knowledge Discovery in Databases*, pages 598–613. Springer.

Scott, J. G. and Berger, J. O. (2010). Bayes and empirical-Bayes multiplicity adjustment in the variable-selection problem. *The Annals of Statistics*, pages 2587–2619.

Shen, W. and Ghosal, S. (2015). Adaptive Bayesian procedures using random series priors. *Scandinavian Journal of Statistics*, 42(4):1194–1213.

Shun, Z. and McCullagh, P. (1995). Laplace approximation of high dimensional integrals. *Journal of the Royal Statistical Society Series B: Statistical Methodology*, 57(4):749–760.

Smith, J. W., Everhart, J. E., Dickson, W., Knowler, W. C., and Johannes, R. S. (1988). Using the ADAP learning algorithm to forecast the onset of diabetes mellitus. In *Proceedings of the Annual Symposium on Computer Application in Medical Care*, page 261. American Medical Informatics Association.

Smith, M. and Kohn, R. (1996). Nonparametric regression using Bayesian variable selection. *Journal of Econometrics*, 75(2):317–343.

Sohn, J., Jeong, S., Cho, Y. M., and Park, T. (2023). Functional clustering methods for binary longitudinal data with temporal heterogeneity. *Computational Statistics & Data Analysis*, 185:107766.

Umlauf, N., Adler, D., Kneib, T., Lang, S., and Zeileis, A. (2015). Structured additive regression models: An r interface to bayesx. *Journal of Statistical Software*, 63(21):1–46.

Wang, L., Liu, X., Liang, H., and Carroll, R. J. (2011). Estimation and variable selection for generalized additive partial linear models. *Annals of Statistics*, 39(4):1827.

Williams, C. and Rasmussen, C. (1995). Gaussian processes for regression. *Advances in Neural Information Processing Systems*, 8.

Womack, A. J., León-Novelo, L., and Casella, G. (2014). Inference from intrinsic Bayes' procedures under model selection and uncertainty. *Journal of the American Statistical Association*, 109(507):1040–1053.

Wood, S. N. (2017). *Generalized Additive Models: an Introduction with R*. CRC press.

Zellner, A. (1986). On assessing prior distributions and Bayesian regression analysis with g-prior distributions. *Bayesian Inference and Decision Techniques: Essays in Honor of Bruno de Finetti*, pages 233–243.

Zellner, A. and Siow, A. (1980). Posterior odds ratios for selected regression hypotheses. *Trabajos de Estadística Y de Investigación Operativa*, 31(1):585–603.